COMPUTER SIMULATION OF VEHICLE MOTION IN THREE DIMENSIONS

I. J. SATTINGER
D. F. SMITH

SPECIAL PROJECTS GROUP
Willow Run Laboratories
THE UNIVERSITY OF MICHIGAN

May 1960

Contracts DA-20-018-ORD-14658 and DA-20-018-ORD-19635

2901-10-T

COMPUTER SIMULATION OF VEHICLE MOTION IN THREE DIMENSIONS

I. J. SATTINGER
D. F. SMITH

May 1960

SPECIAL PROJECTS GROUP
Willow Run Laboratories
THE UNIVERSITY OF MICHIGAN
Ann Arbor, Michigan

This project is carried on for the Ordnance Tank-Automotive Command under Army Contract Numbers DA-20-018-ORD-14658 and DA-20-018-ORD-19635. University contract administration is provided to Willow Run Laboratories through The University of Michigan Research Institute.

Delivered by The University of Michigan pursuant to Contract No. DA-20-018-ORD-19635. Government's use controlled by General Provision 27 of the contract which is ASPR 9-203.1 and ASPR 9-203.4 (Revised 15 October 1958).

CONTENTS

FIGURES

TABLES

SYMBOLS

Coordinate Systems (see Figure 23)

$\bar{i}$, $\bar{j}$, $\bar{k}$	Unit vectors in the body-fixed coordinate system
x, y, z	Coordinate axes in the body-fixed coordinate system
$\bar{i}'$, $\bar{j}'$, $\bar{k}'$	Unit vectors in the earth-based coordinate system
x', y', z'	Coordinate axes in the earth-based coordinate system

Euler Angles (see Figure 25)

A	Azimuth angle
E	Elevation angle
B	Bank angle

Suspension and Tire Force Functions

K_{ns}	Suspension-spring force-vs.-displacement function for the n-th wheel
C_{ns}	Shock-absorber force-vs.-velocity function for the n-th wheel
ϕ_{ns}	Shock-absorber force-vs.-displacement function for the n-th wheel
K_{nw}	Tire spring force-vs.-displacement function for the n-th wheel
C_{nw}	Tire damping force-vs.-velocity function for the n-th wheel
ϕ_{nw}	Tire damping force-vs.-displacement function for the n-th wheel

Other Symbols

a	Acceleration
c_{lm}	Direction cosine between the l and m axes where l = i, j, k and m = i', j', k'
CG	Center of gravity
F	Force
$\bar{F}_n$	Vector of force acting on the body from the n-th wheel
F_{ni}, F_{nj}, F_{nk}	i, j, and k components of $\bar{F}_n$
$\bar{g}$	Gravity vector
g	Magnitude of $\bar{g}$
$\bar{G}_n$	Vector of the ground-reaction force on the n-th wheel
G_{ni}, G_{nj}, G_{nk}	i, j, and k components of $\bar{G}_n$
$\bar{H}_n$	Angular momentum vector of the n-th wheel
$\bar{H}_o$	Angular momentum vector of the body
J	Moment of inertia
J_a	Pitch moment of inertia of the body about the axle

SYMBOLS (Continued)

J_{ni}, J_{nj}, J_{nk}	Moments of inertia of the n-th wheel about the i, j, and k axes through the wheel hub
J_{oi}, J_{oj}, J_{ok}	Moments of inertia of the body about the i, j, and k axes through the CG
K	Factor by which the roll moment of inertia is increased (see Equation 1)
m	Mass
m_q	Mass of the q-th particle
m_n	Mass of the n-th wheel
m_o	Mass of the body
$\bar{M}_n$	Vector of moments acting on the n-th wheel
$\bar{M}_o$	Vector of moments acting on the body
M_{oi}, M_{oj}, M_{ok}	i, j, and k components of $\bar{M}_o$
P_{oij}, P_{oik}, P_{ojk}	Products of inertia of the body
r	Distance from the rear axle to the CG
$\bar{r}_q$	Position vector of the q-th particle from the body's CG
$\bar{r}_n$	Position vector of the n-th wheel from the origin of the earth-based coordinate system
r_{ni}, r_{nj}, r_{nk}	i, j, and k components of $\bar{r}_n$
$\bar{r}_{ng}$	Position vector of the n-th wheel's ground-contact point from the origin of the earth-based coordinate system
r_{ngi}	i component of $\bar{r}_{ng}$
$r_{ngi'}$, $r_{ngj'}$, $r_{ngk'}$	i', j', and k' components of $\bar{r}_{ng}$
$\bar{r}_{nw}$	Position vector of the n-th wheel's ground-contact point from the wheel hub
r_{nw}	Magnitude of $\bar{r}_{nw}$
$\bar{r}_o$	Position vector of the body's CG from the origin of the earth-based coordinate system
r_{oi}, r_{oj}, r_{ok}	i, j, and k components of $\bar{r}_o$
$r_{oi'}$, $r_{oj'}$, $r_{ok'}$	i', j', and k' components of $\bar{r}_o$
R_w	Radius of the wheel from hub to tire tread
T	Torque
$\bar{T}_n$	Vector of torque acting on the n-th wheel
T_{ni}, T_{nj}, T_{nk}	i, j, and k components of $\bar{T}_n$
[T]	Coordinate transformation matrix (see Section A.7)
V	Forward velocity of the vehicle
v	Velocity

SYMBOLS (Continued)

v_q	Inertial velocity of the q-th particle
x_q, y_q, z_q	x, y, and z coordinate of the q-th particle from the body's CG
X_n, Y_n, Z_n	x, y, and z coordinates of the n-th wheel from the body's CG
x_o, y_o, z_o	x, y, and z coordinates of the body's CG from the origin of the earth-based coordinate system
x_o', y_o', z_o'	x', y', and z' coordinates of the body's CG from the origin of the earth-based coordinate system
z_n	Displacement of the n-th wheel from the neutral position of the suspension
θ_{oi}	Pitch angle of the body
θ_{oj}	Roll angle of the body
μ	Coefficient of friction
ω	Angular velocity
$\bar{\omega}_o$	Vector of the angular velocity of the body
ω_{oi}, ω_{oj}, ω_{ok}	i, j, and k components of $\bar{\omega}_o$
$\bar{\omega}_n$	Vector of the velocity of the n-th wheel
ω_{ni}, ω_{nj}, ω_{nk}	i, j, and k components of $\bar{\omega}_n$

Dot (·) or double dot (··) over a symbol denotes derivatives with respect to time.

COMPUTER SIMULATION OF VEHICLE MOTION IN THREE DIMENSIONS

ABSTRACT

This report describes the results of a research program to develop techniques of simulating three-dimensional motion of a vehicle by means of electronic computers. In order to provide the basis for vehicle-motion simulation, a complete set of equations for a wheeled vehicle was developed, which permitted the analysis of motion in pitch, yaw, roll, bounce, surge, and sideslip. The derivation and summary of these equations is presented in this report. As a means of reducing the time and cost of computer solutions for certain restricted cases of vehicle motion, an investigation was made to determine to what extent simplifying assumptions could be made in these equations. A simplified set of equations is contained in the report for cases in which surge can be neglected and angular motions in pitch and roll do not exceed 10°. A second simplified set of equations contains the further restriction that only pitch, bounce, and roll occur.

In order to establish justification for the simplified equations, an experimental program was carried out on an XM-151 military truck to determine its motion when traveling over certain road obstacles under specified conditions. The results were compared with those of corresponding runs in an analog-computer simulation. It was concluded that the simplified equations allowing only for pitch, bounce, and roll motion gave a satisfactory representation of the field-test data, but that improved correlation could be obtained by the simplified set of equations which accounted for lateral motion as well.

1 INTRODUCTION[1]

This report describes the results of a research program, undertaken by Willow Run Laboratories of The University of Michigan, to develop techniques of simulating three-dimensional

[1]The authors wish to acknowledge the work of B. Herzog and D. Y. Liang in connection with this research program. Mr. Herzog assisted in the derivation of the complete set of equations of vehicle motion, as presented in Appendix A. Mr. Liang was responsible for preparing, checking, and operating the analog-computer setup discussed in Section 3.

motion of a vehicle by means of an analog computer. The work described here is a direct outgrowth of previous research projects, sponsored by the Ordnance Tank-Automotive Command, in which methods of simulating vehicle motion in two dimensions were developed (Reference 1). The application of these original studies is confined to analyses involving angular motion of the body of the vehicle about its transverse axis (pitch), translational motion in a vertical direction (bounce), and translational motion in a longitudinal direction (surge).

The simulation of vehicle motion by means of electronic computers provides an important method of analyzing certain types of vehicle-design problems. Examples of such problems which occur in connection with military-vehicle design are investigations of the effect of suspension-system design on ride characteristics, and of the stability of the vehicle in the presence of gun-recoil forces.

The specific objectives of this program were:

(1) To develop a generalized mathematical model which can be used for the investigation of design problems involving vehicle motion. The equations composing this model should represent both angular motion of the vehicle (including pitch, roll, and yaw) and translational motion (including bounce, sideslip, and surge).

(2) From this general mathematical model, to obtain simplified versions of the equations suitable for design studies involving motion only in pitch, bounce, roll, and sideslip.

(3) To establish the validity of these simplified equations by comparing data obtained from field tests on a real vehicle with results obtained by the use of the equations in a corresponding analog-computer simulation.

The investigation described in this report has been based on a field-test program and computer simulation of a four-wheeled vehicle. However, the mathematical model has been prepared for vehicles having any number of wheels and can be applied, with some modification, to articulated vehicles. The model is also adaptable to track-laying vehicles. For certain types of problems, forces applied to the hull by the track (for example, due to accelerating or braking) significantly affect the motion; in such cases, the equations must be modified to include the effect of these forces.

2
DERIVATION of THREE-DIMENSIONAL EQUATIONS

2.1. COMPLETE SOLUTION OF EQUATIONS OF MOTION

As the basis for the development of the three-dimensional simulation of a vehicle, the equations of motion were derived for a wheeled vehicle whose body is free to move in three

degrees of angular freedom and three degrees of translational freedom. The three quantities representing translational displacement are designated sideslip (x_o'), surge (y_o'), and bounce (z_o'); the three quantities representing rotational displacement are designated azimuth (A), elevation (E), and bank (B). Corresponding angular velocities are designated yaw (ω_{ok}), pitch (ω_{oi}), and roll (ω_{oj}), respectively. The equations define the motion of the body of the vehicle and of each wheel as affected by the force of gravity, the interactions between the body and the wheels, and the reactions of the ground (including the effect of longitudinal forces produced by the engine and brakes).

The complete solution of the equations of motion can provide the displacement, velocity, and acceleration as a function of time of the body and of each wheel in each of the six degrees of freedom. It can also provide a time record of the forces acting on each of these objects.

The motion of an object subject to a combination of forces and torques is governed by Newton's laws of motion. For each part of the vehicle (such as the body or each wheel), an equation can be written to determine linear acceleration along each of three coordinate axes which are fixed with respect to the earth. These three equations are of the form:

$$\Sigma F = ma$$

where ΣF = sum of all forces acting on the object along a given axis

m = mass of the object

a = acceleration of the object along the given axis

Similarly, for each part of the vehicle, an equation can be written to determine angular acceleration along each coordinate axis. These equations are of the form:

$$\Sigma T = J\dot{\omega}$$

where ΣT = sum of all torques acting on the object around a given axis

J = moment of inertia of the object around the axis

$\dot{\omega}$ = angular acceleration around the axis

In order to derive velocity and position information from the above equations which define acceleration, integral equations are required of the general form:

$$v = \int a\,dt \quad \text{and} \quad x = \int v\,dt$$

The body is acted on by two types of force. One is the force of gravity; the other is the summation of forces applied to the body by the suspension components of each wheel, that is, by the spring and shock absorber. In the case of a track-laying vehicle, additional forces on the body would be produced by the tracks themselves. In the present analysis, however, a wheeled vehicle is assumed.

In addition to equations describing the motion of the body, equations are required for the motion of each wheel. It may be assumed without appreciable error that the motion of the wheel with respect to the hull is confined to a straight line parallel to the yaw axis. The motion of each wheel is the result of the force of gravity, the reaction from the ground acting through the tire, and forces exerted by the suspension spring and shock absorber.

It is convenient to write the equations of motion of the hull and of each wheel in terms of body-fixed axes, that is, a set of axes parallel to the pitch, yaw, and roll axes of the body. On the other hand, the output quantities representing translation and rotation of the body, and the profile data on the road over which the vehicle travels are best represented in terms of a set of earth-based axes. Consequently, a number of coordinate-transformation equations are required which relate displacement, velocity, and acceleration in terms of earth-based axes to corresponding quantities in terms of the body-fixed axes.

In general terms, then, it is possible to say that the simulation of vehicle motion in three dimensions involves the solution of a set of equations consisting of the following types:

(1) Equations representing Newton's laws of motion for both rotational and translational effects of the body and of each wheel.
(2) Equations representing forces transmitted by springs, shock absorbers, and tires as functions of wheel displacement and velocity with respect to the body or to the ground.
(3) Coordinate-transformation equations relating displacements, velocities, or accelerations in body axes to those in earth-based axes.

The detailed derivation of the complete equations of motion of a wheeled vehicle in three dimensions is presented in Appendix A. In the derivation, the following simplifying assumptions were made:

(1) The vehicle is assumed to be symmetrical about the plane of the yaw and roll axes.
(2) Motion of each wheel with respect to the body is assumed to follow a straight line parallel to the yaw axis of the vehicle.
(3) Each tire is assumed to make contact with the ground at a point on the straight line of travel of the wheel hub.
(4) Reaction on the body of the vehicle and due to engine rotation is neglected.

Using the set of equations as derived in Appendix A, rough estimates were made of the amount of analog-computer equipment which would be required to represent these equations. It was determined that, to represent the motion of a four-wheeled vehicle, the total analog equipment required would consist of approximately 160 operational amplifiers, 17 multipliers, and 16 function generators. For an eight-wheeled vehicle the amount of equipment required increases to 275 operational amplifiers, 22 multipliers, and 32 function generators. Since the time, cost, and complexity of a computer solution increase with the quantity of equipment required, it was considered desirable to determine to what extent simplifying assumptions

could be made which would reduce the complexity of the equations and minimize the equipment required. There are numerous possibilities for making such simplifications, but it is important to avoid incurring excessive error in doing so.

2.2. SIMPLIFICATION OF EQUATIONS

In Appendix B, the equations developed in Appendix A are rewritten utilizing certain simplifying assumptions. Several simplifications are made to write the equations of Section B.1; and then one additional simplification is made to write the equations of Section B.2. The simplifications used for the equations of Section B.1 are as follows:

(1) The results of field tests show that the forward velocity of a vehicle is very nearly constant even when the vehicle is travelling over a fairly rough road (Figure 21). Hence the equations pertaining to the forward motion of the vehicle are replaced by the proposition that the vehicle's forward velocity is constant.

(2) When only small angles of motion of the body need be considered, it is possible to set the direction cosines between corresponding directions in the earth-based and body-fixed coordinate systems equal to 1 and all other direction cosines equal to 0. Since many practical cases of vehicle motion are those in which pitch, roll, and yaw angular deviation from a mean value do not exceed 5^{o} or 10^{o}, such a simplifying assumption appears to be reasonable.

(3) Certain of the mathematical terms that appear in the equations as a result of working in body axes represent gyroscopic effects and centrifugal-force effects, which result from rotations of the body. It is possible by inserting typical values of these rotational velocities to establish the validity of omitting these terms.

In the equations given in Section B.2, one additional simplification is made: sidewise motion, sideslip, is omitted. This set of equations restricts the motion of the body to only three of the six degrees of freedom, specifically, to pitch, bounce, and roll. This restriction naturally limits the scope of the problems which can be investigated by means of the simplified simulation; however, many problems of interest can be studied in this manner without serious loss of realism. For example, studies of the ride characteristics of automotive vehicles can be confined to the interpretation of pitch, bounce, and roll motion, since these components of the total motion tend to be the most pronounced.

In order to determine the feasibility of developing simplified versions of the complete system of equations, the set of equations of Section B.2 was investigated in detail. By restricting the problem in this manner it was possible to make a computer setup requiring only 52 operational amplifiers and 16 function generators. No multipliers were required. The functions

to be represented are those of the nonlinear force-vs.-motion characteristics of the suspension components. By making the additional assumption that each of these characteristics is composed of two or three linear segments, it is possible to accomplish the function-generation process in a simple manner, that is, by the use of additional operational amplifiers with nonlinear feedback rather than by the use of conventional function generators. The details of this computer setup are discussed in Section 3.2.

3
FIELD-TEST and SIMULATION PROGRAMS

In order to establish justification for the simplified version of the vehicle-motion equations developed in Section B.2 as well as to gain experience in their use, an experimental program was carried out involving both a computer study and a series of field tests. Data were obtained from a computer set up for a number of runs of a Ford Motor Company XM-151 military utility transport truck (an experimental four-wheeled vehicle similar to a jeep) when triangular ramps of various sizes and spacings were traversed. In order to check the validity of this computer setup, a field-test program was conducted in which an XM-151 was instrumented by means of accelerometers, gyroscopes, and wheel-position-measuring potentiometers. Runs were made over road obstacles consisting of triangular ramps at speeds corresponding to those used in the computer tests. The field test and computer data could then be compared for what should be identical conditions to determine the accuracy of the simulation and to establish permissible simplifying assumptions.

3.1. DESCRIPTION OF THE FIELD-TEST PROGRAM

The XM-151 was selected for the field-test program for the following reasons:

(1) The use of a four-wheeled vehicle would require the least complication in terms of the total instrumentation required, and the magnitude of the corresponding computer setup, without limiting the validity of the results.
(2) Since the Ford Motor Company had used this same type of vehicle for certain analog-computer studies, some data concerning vehicle system parameters were available which would be useful in carrying out the program described here.

The vehicle, whether real or simulated, traveled at identical speeds over a road containing identical road irregularities, and the corresponding real and simulated data in pitch, bounce, and roll motion were to be compared in order to determine how accurately the real motion was simulated on the computer. In order to make this comparison, it was decided to measure and

record the following quantities:

(1) Pitch, bounce, and roll velocities
(2) Bounce and sideslip accelerations
(3) Pitch, roll, and yaw angles
(4) Position and velocity of each wheel with respect to the body

The test runs consisted of running the vehicle at various speeds along a concrete road on which were located a number of triangular obstacles. The dimensions of the obstacles and the particular arrangement of obstacles along the path are shown in Figure 1. Each arrangement is designated by a case number. Table I shows the speeds and indicates obstacle arrangements for the field tests.

The yaw, pitch, and roll angles were most easily measured by the use of motion-picture camera techniques. A camera was set up at a distance of about 100 feet from the side of the road and approximately in line with the road obstacles. Another camera was set up looking along the road. In order to permit measurement of the angular and translational motion of the body of the vehicle, markers were attached to it and a fence was constructed along the side of the road to provide reference positions against which the vehicle position could be measured from frame to frame of the motion-picture record. This technique has been discussed in

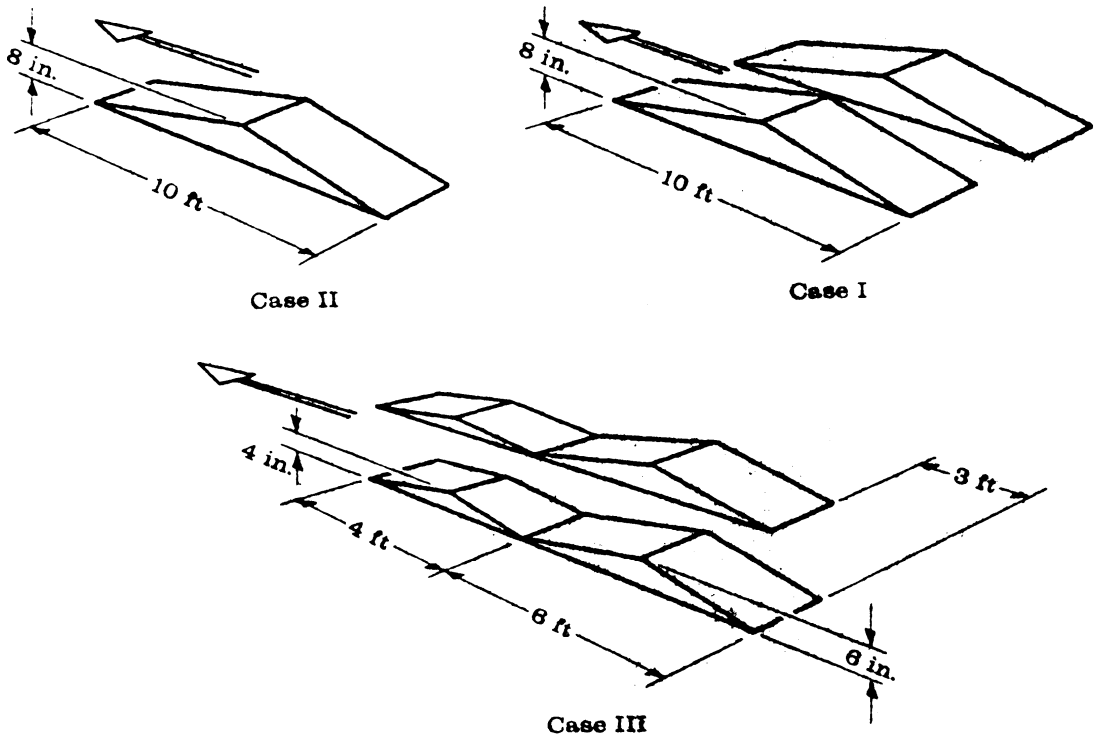

FIGURE 1. ROAD CONFIGURATION

TABLE I. FIELD-TEST CONDITIONS

Run Number	Case Number	Speed (fps)
1	I	12.1
2	I	16.1
3	II	10.7
4	II	15.2
5	II	22.1
6	III	16.7
7	III	23.6

greater detail in Reference 1. Figure 2 shows the setup used for the field tests. The vertical poles on the jeep were used to measure pitch, roll, and yaw angles, and the fence in the foreground was used as a horizontal reference for measurements. The obstacles are shown in position for a Case III run.

Angular velocities of the body were measured by means of three rate-gyros rigidly attached to the body. The sensitive axes of these three gyros were so aligned with respect to the vehicle body axes as to give a continuous indication of pitch, yaw, and roll velocities.

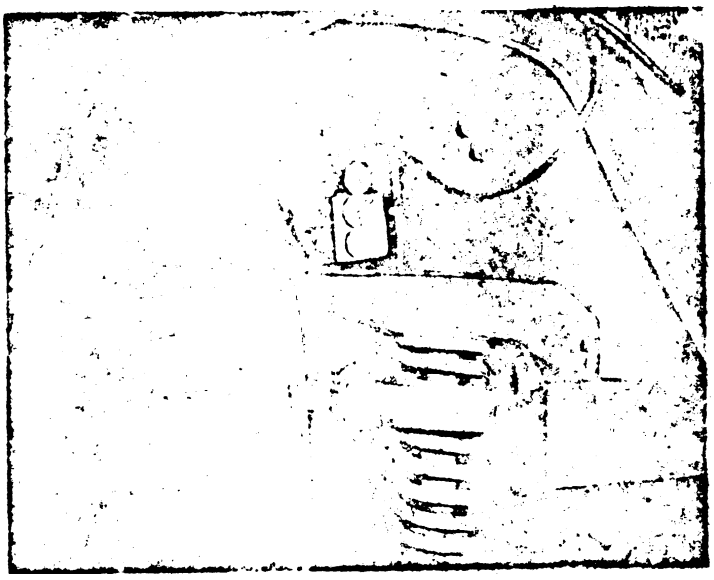

FIGURE 2. FIELD-TEST SETUP, GENERAL VIEW

Accelerations were measured by means of two accelerometers which were mounted on the frame of the vehicle with their sensitive axes aligned along the vertical and longitudinal vehicle axes. These accelerometers were located at the center of gravity of the body so that the accelerations measured were always those occurring at this point. Figure 3 shows the gyros and accelerometers mounted in the jeep. The accelerometers are shown mounted on the CG marker which is above the transmission, and the gyros are mounted on the platform behind the front seat. This platform also served as a distribution center for the electrical cables to the various instruments.

The motion of each wheel with respect to the body was measured by means of an assembly, shown in Figure 4, attached to the body frame. The assembly contained a potentiometer and a tachometer for measuring wheel extension and wheel velocity, respectively. These devices could be rotated by means of a small steel cable attached to their shafts by means of a pulley arrangement. The end of the cable was attached to the upper wishbone of the suspension. Downward motion of the wheel extended the cable, and upward motion of the wheel permitted a rewind spring to retract the cable. This motion transmitted to the potentiometer and tachometer produced the desired electrical outputs.

In order to provide permanent records of the field-test data, the outputs of all rate gyros, accelerometers, and wheel-measuring devices were routed through amplifiers to a recording oscillograph that had provisions for up to 14 channels of data. Synchronization between the oscillographic data and the motion-picture data was obtained by means of an event-marker

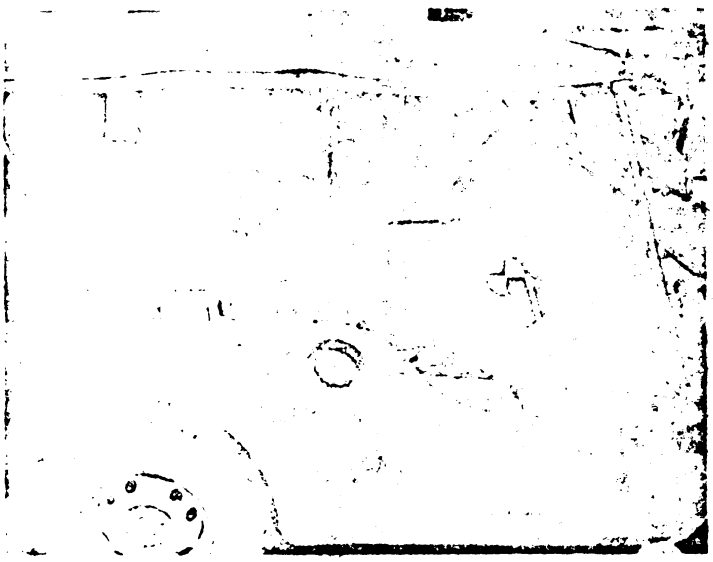

FIGURE 3. FIELD-TEST SETUP, VEHICLE INTERIOR

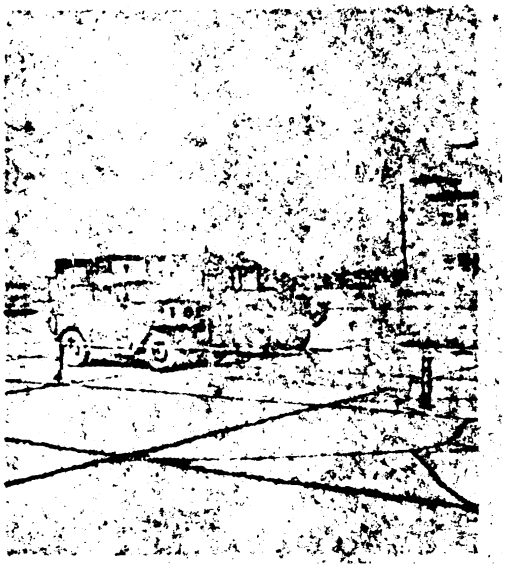

FIGURE 4. WHEEL POSITION AND VELOCITY-MEASURING DEVICE

system. This started the timing lines on the oscillograph at the same instant that a flash bulb was set off in view of the camera.

During the test runs, the amplifiers, recording oscillograph, and power supplies were carried aboard an M4 ambulance which ran alongside the jeep (Figure 5). Interconnections between the ambulance and jeep were made by a set of electrical cables which are shown entering the ambulance from behind the front seat in Figure 5 and are shown on the far side of the jeep in Figure 3. Electric power was supplied by an engine-driven a-c generator mounted on the front of the ambulance (Figure 2).

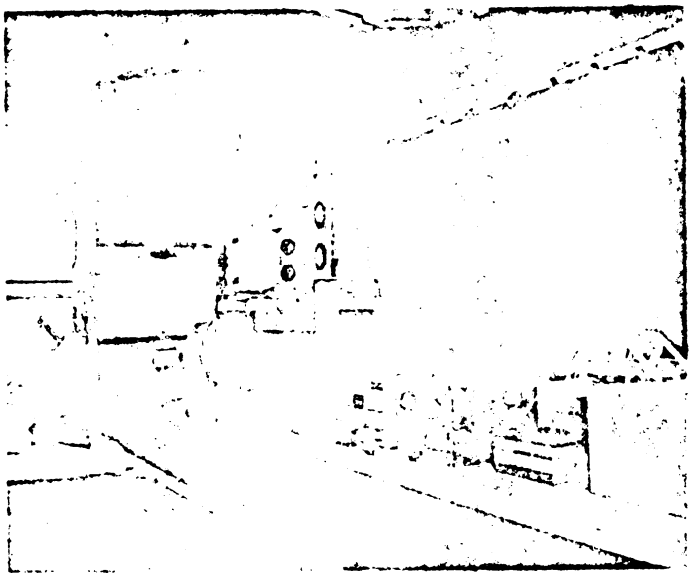

FIGURE 5. FIELD-TEST SETUP, INSTRUMENT-TRUCK INTERIOR

3.2. ANALOG-COMPUTER INVESTIGATION

The analog computer at Willow Run Laboratories was set up, using the equations in Section B. 2, to simulate the XM-151 military truck. This setup included 56 operational amplifiers of which 8 used nonlinear feedback to represent the suspension springs and the effects of the tires leaving the ground. The computer diagram for the simulation, which was run in one-tenth real time, is shown in Figure 6. The main component of the road-function generator is a ganged stepping switch, each gang being used for the road input to one particular wheel. The output of each step is a voltage which represents the slope of the road; each step represents 1 foot of travel along the road. The stepping rate, which is controlled by an audio-oscillator, then represents the speed of the vehicle. The vehicle speeds and road configurations simulated are the same as those under which field tests were run.

In order to make the series of analog-computer runs, it was necessary to determine the magnitudes of the vehicle-design constants which are used as parameters of the equations. Table II shows the constants used and their values. The methods used to determine these values follow.

To obtain the spring rate of the front suspension springs, the wheels and shock absorbers were removed and the body was blocked up so that it was free to pivot about the rear axle. A known weight was placed directly over the front axle, and the displacement of the front wheel hubs with respect to the body was measured. Since the two front springs are in parallel, the rate of each spring is equal to one-half this computed value. The procedure was repeated with the rear wheels to determine the constant of their suspension springs. The force-vs.-deflection curves for the front and rear springs are shown in Figures 7 and 8. The static position and positions of metal-to-metal contact in jounce and rebound were found by removing the suspension spring and measuring the wheel displacement when it was at the various positions. This was also done with the rear wheels to determine the point of contact with the rubber bump stop.

In order to determine the unsprung mass of each wheel, the body was blocked up so that the wheel hung free. The shock absorber and suspension spring were removed, and a different spring of known spring rate was installed. The wheel was lifted and released, and its transient motion was recorded by means of the wheel-measuring potentiometer described in Section 3.1. Assuming the system to be governed by a second-order differential equation, the measurement of the period of oscillation permitted the calculation of the unsprung mass.

A set of measurements was made to determine the distribution of the total vehicle weight among the four wheels. The sum of the individual weights on each wheel gives the total vehicle weight. By subtracting the sum of the unsprung masses at each wheel, the sprung mass was obtained. The weight distribution in conjunction with the values of wheelbase and track width could then be used to calculate the location of the center of gravity of the sprung mass in a horizontal plane. Thus, the values of Y_1, Y_2, Y_3, Y_4, X_1, X_2, X_3, and X_4 could be computed.

The vertical position of the CG was not measured, but was available from measurements previously made by the Ford Motor Company. This particular value is not used in the simplified equations studied on the computer.

The moment of inertia of the body in pitch was determined by a test for which the vehicle was blocked up in the same manner that was used to measure the front spring rate (i.e., the body was pivoted about the rear axle with the front suspension springs in place). Oscillations were induced by dropping the front end of the vehicle, forcing it to rotate about an axis parallel to the pitch axis, with springing supplied by the front suspension springs. Based on the known spring rate and the observed period of oscillation, the pitch moment of inertia around the rear

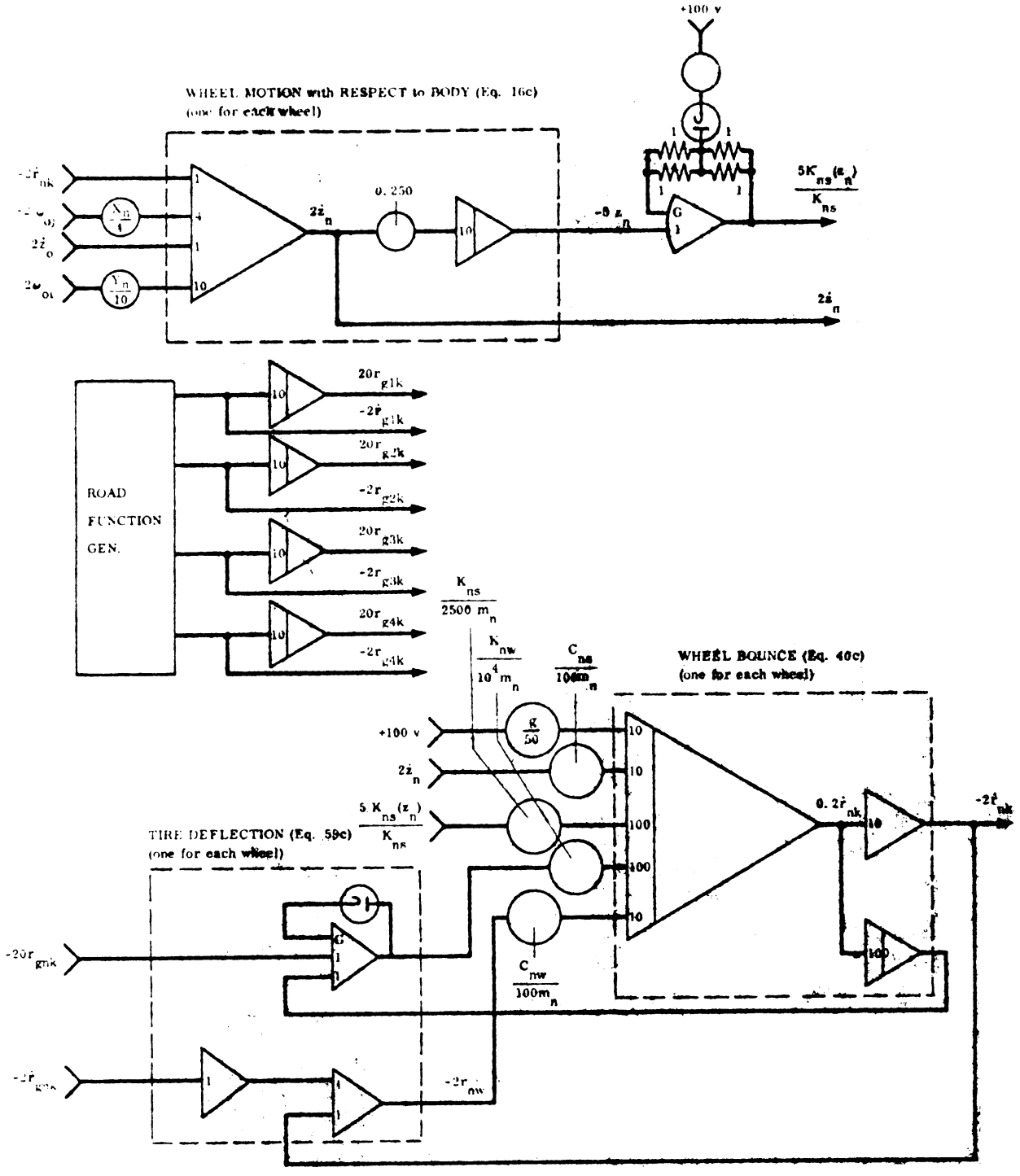

FIGURE 6. COMPUTER DIAGRAM

Notes: (1) Problem is run in one-tenth time. Gain shown on integrators is actual gain of the variable through the integrator. (2) Y_2, Y_4, X_3, and X_4 are negative quantities.

BODY BOUNCE (Eq. 20c)

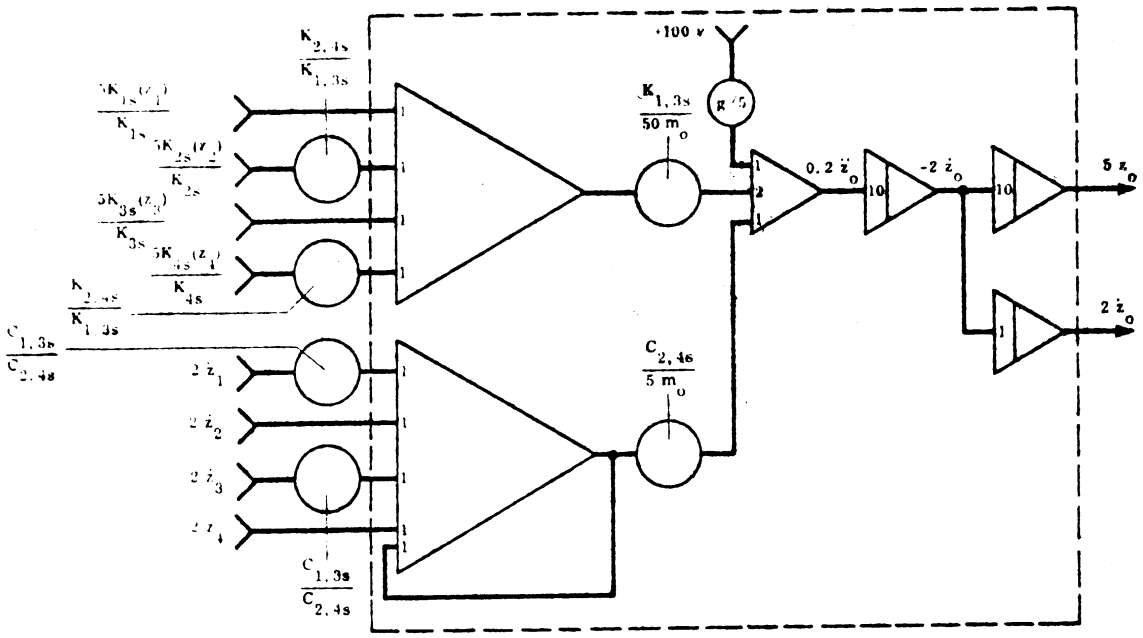

BODY ROLL (Eq. 35c)

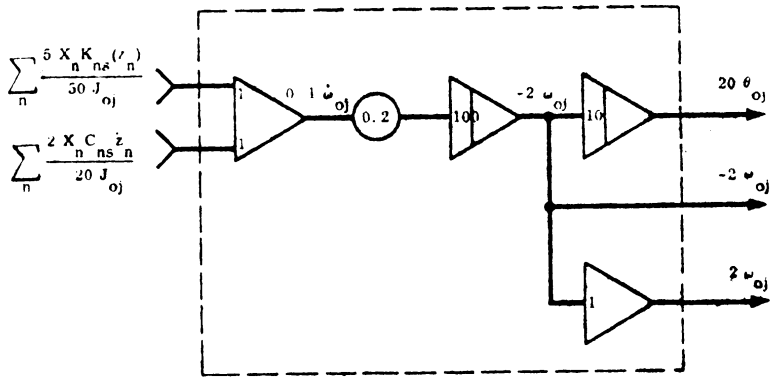

BODY PITCH (Eq. 34c)

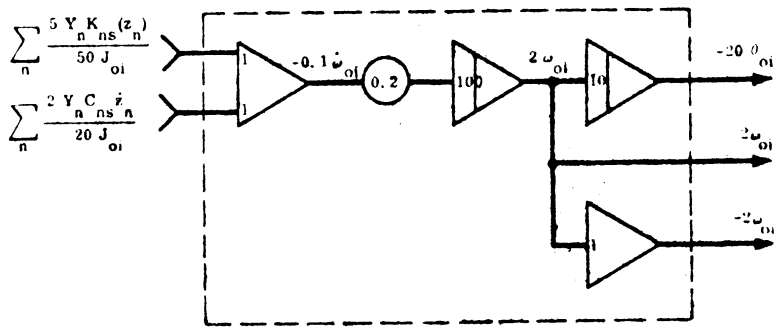

TABLE II. CONSTANTS USED FOR SIMULATION*

Symbol	Value	Description
J_{oi}	461.1 lb-ft-sec^2	Pitch moment of inertia
J_{oj}	84.0 lb-ft-sec^2	Roll moment of inertia
m_o	59.1 slugs	Mass of the body
m_1, m_3	2.56 slugs	Mass of front wheel
m_2, m_4	1.87 slugs	Mass of rear wheel
Y_1, Y_3	3.07 ft	Fore and aft distance of wheel from CG
Y_2, Y_4	-4.01 ft	
X_1, X_2	-1.07 ft	Transverse distance of wheel from CG
X_3, X_4	1.07 ft	
K_{1s}, K_{3s}	1697 lb/ft	Spring constant of suspension springs
K_{2s}, K_{4s}	1557 lb/ft	
C_{1s}, C_{3s}	119 lb/ft/sec	Shock absorber force vs. rate
C_{2s}, C_{4s}	163 lb/ft/sec	
K_{1w}, K_{3w}	8100 lb/ft	Tire spring rate
K_{2w}, K_{4w}	11,000 lb/ft	
C_{1w}, C_{3w}	7.9 lb/ft/sec	Tire force vs. rate
C_{2w}, C_{4w}	8.3 lb/ft/sec	

*Wheel number convention: 1, left front; 2, left rear; 3, right front; 4, right rear.

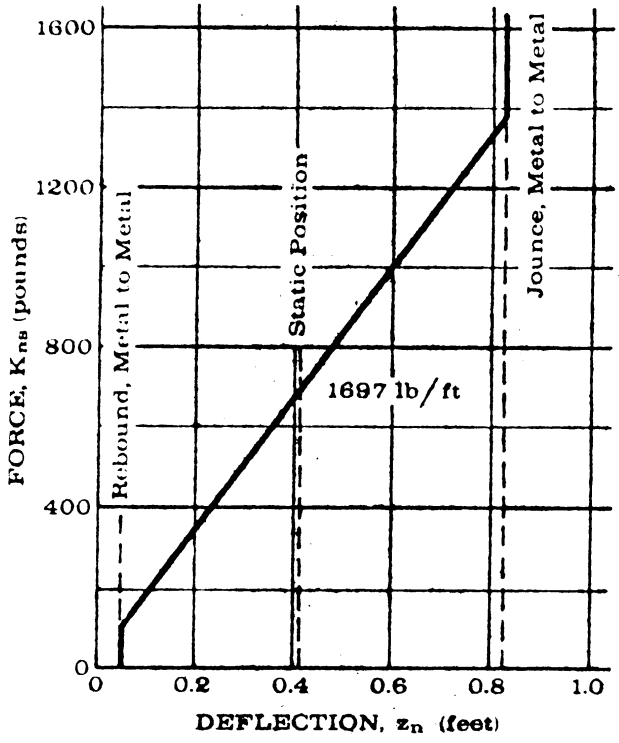

FIGURE 7. FRONT-SPRING FORCE VS. DEFLECTION. Front spring viewed at hub.

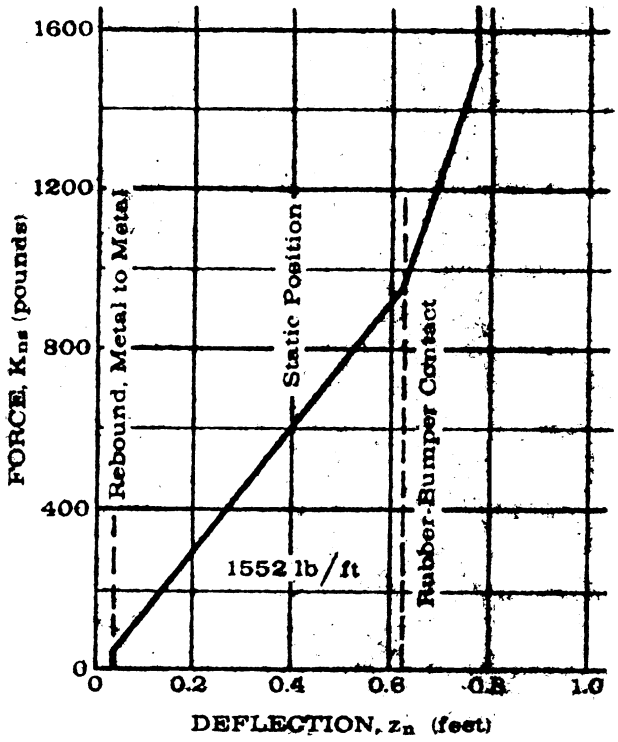

FIGURE 8. REAR-SPRING FORCE VS. DEFLECTION. Rear spring viewed from hub.

axle could be computed. The moment of inertia around the pitch axis through the center of gravity could then be computed by means of the equation

$$J_{oi} = J_a - m_o r^2$$

where J_a = measured moment of inertia about the axle

r = distance from the pitch axis through the axle to the pitch axis through the CG

To serve as a check, this type of measurement was repeated for motion pivoting about the front axle, and it was found that the two computed values of J_{oi} were close to agreement. For the measurement of roll moment of inertia J_{oj}, the same type of measurement was performed with the vehicle blocked up on one side.

To check the analog-computer setup, the tests performed on the vehicle to determine the moments of inertia were simulated on the computer. The blocked wheels of the vehicle were simulated by taking a very high value for the spring constants of these wheels. Table III shows the periods of oscillation which were observed on the vehicle tests and the corresponding periods observed for the computer simulation of these tests.

The damping constant of the system due to the presence of shock absorbers and of other sources of friction was found in a test similar to that described for the moments of inertia,

TABLE III. COMPARISON OF ACTUAL AND SIMULATED PERIODS OF OSCILLATION

Test	Period of Oscillation (sec)		Deviation (%)
	XM-151	Computer	
Roll	0.525	0.520	0.95
Pitch			
Front Blocked	0.525	0.511	3.0
Rear Blocked	0.587	0.577	1.7

but with the shock absorbers in place. The front or rear axle of the vehicle was placed on blocks, caused to oscillate, and its motion recorded by the wheel-measuring potentiometers. Because of the high degree of damping, it was impossible to determine a rate of oscillation decrement. However, by means of a technique described in Reference 2, the damping constant could be determined from the shape of the overdamped transient. The shock-absorber force-vs.-velocity curves determined by this method are shown in Figures 9 and 10. Since the damping constants for the shock absorbers are nearly the same for both positive and negative velocities, linear shock absorbers with the damping constant shown in the first quadrant of the figures were used in the simulation.

The spring and damping characteristics of the tire were taken from data supplied by the Ford Motor Company.

3.3. COMPARISON OF FIELD-TEST AND SIMULATION RESULTS

As the basis for evaluating the adequacy of the computer simulation using the equations of Section B.2, the results of the XM-151 field tests were compared with the computer simulation for the seven runs listed in Table I. The evaluation of this comparison is discussed in this section.

In reviewing the results, the determination of cause of any discrepancies between real and simulated data will be attempted. One possible source of discrepancy is the presence of errors in the field-test data, due to limitations in the accuracy of the data-collection devices and methods. In addition, there were difficulties in controlling some of the conditions under which the field tests were run (e.g., smooth road, constant speed, and no sideslip) so that they correspond to the conditions assumed in the computer simulation. Discrepancies due to these causes do not indicate any limitation of the computer representation. On the other hand, any discrepancy which is due to oversimplification of the equations must be taken as an indication

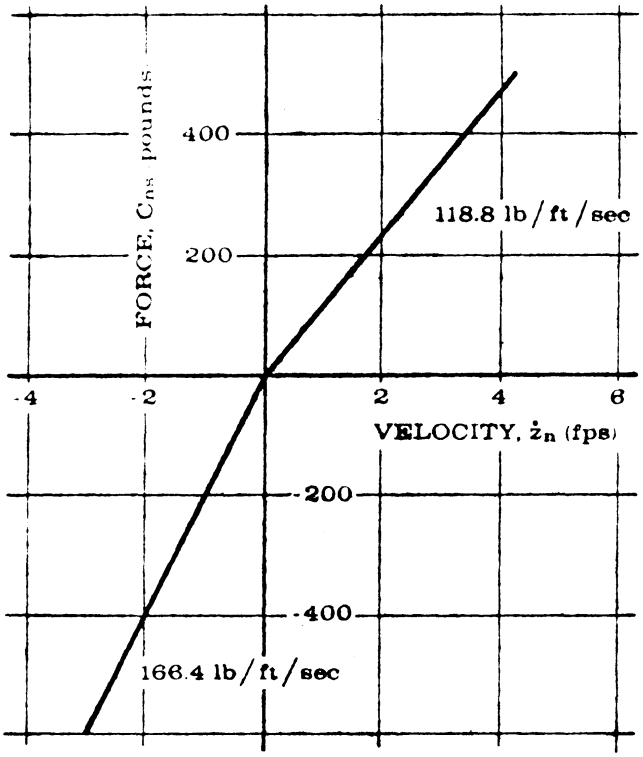

FIGURE 9. FRONT-SHOCK-ABSORBER FORCE VS. VELOCITY. Front shock absorber viewed from hub.

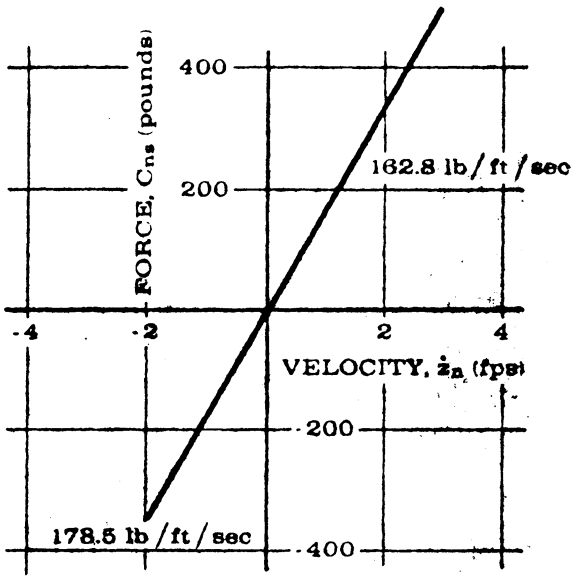

FIGURE 10. REAR-SHOCK-ABSORBER FORCE VS. VELOCITY. Rear shock absorber viewed from hub.

of the need to include additional features in the simulation. In the following discussion, some estimates of the source of discrepancies can be given, but due to limitations of time available for the analysis it has not been possible to indicate the exact reason for all differences between real and simulated data.

Some general observations can be made concerning sources of discrepancies, before the individual runs are reviewed. It is believed that errors in the field-test data may range up to 0.1 ft for bounce (z_0 and z_1), and 0.02 rad for pitch angle (θ_{oi}) and roll angle (θ_{oj}). Consequently, discrepancies of less than these amounts may be due to experimental error and are not significant.

The assumption that the jeep moved at constant velocity was checked by using the movie data to plot distance vs. time. The data for Runs No. 1, 5, and 7 are shown in Figure 11. The fact that the slope of each curve is substantially constant indicates that this is a good assumption.

The importance of centrifugal and gyroscopic terms in the equations was investigated by reading out of one of the computer runs certain products of angular velocities which enter into such terms. The magnitude of these products is shown in Figure 12 in comparison with the angular acceleration terms, $\dot{\omega}_{oi}$ and $\dot{\omega}_{oj}$. It can be seen that the velocity-product terms are in

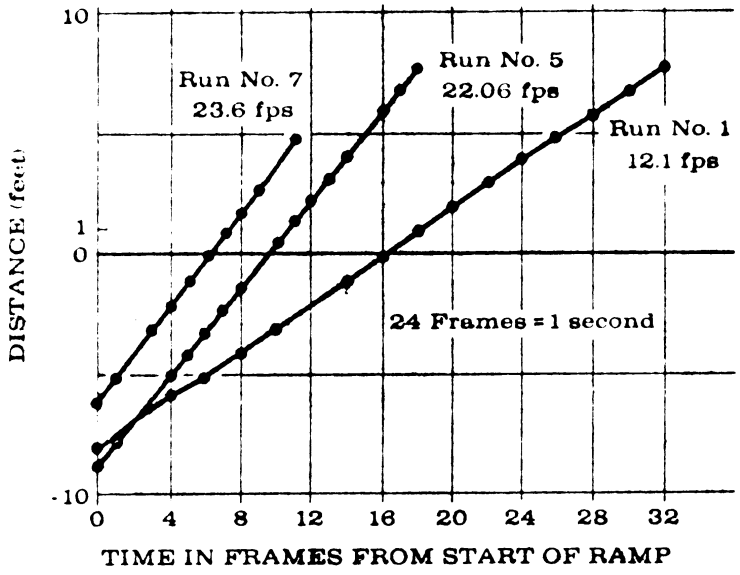

FIGURE 11. CALCULATED FORWARD VELOCITY

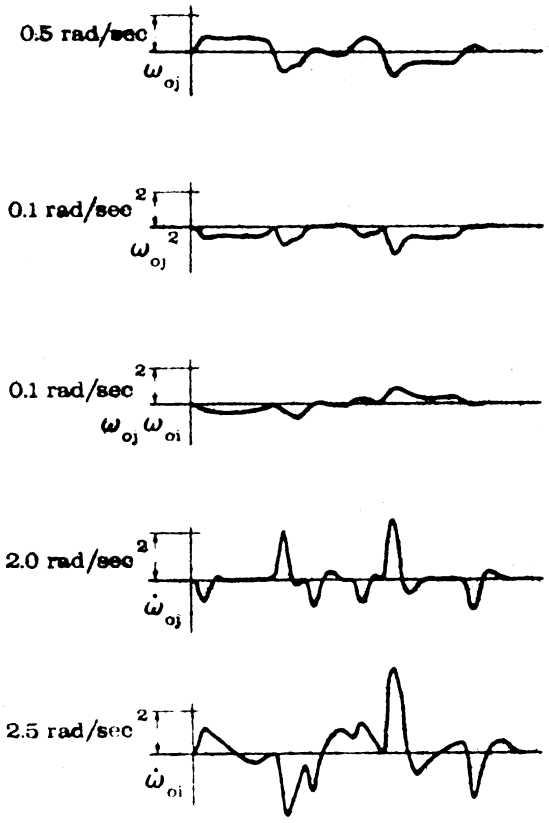

FIGURE 12. COMPARISON OF GYROSCOPIC AND CENTRIPETAL ACCELERATION TERMS

general much smaller than the acceleration terms, indicating that the error introduced into the equations by neglecting these terms is correspondingly small.

In most of the runs, the pitch angle of the vehicle throughout the run has an increasingly negative bias and the height of the body CG drifts downward slightly. This may indicate that the concrete road was not perfectly level. If the field-test data were modified to remove the bias noted, the comparison with the simulated data would be somewhat improved.

The comparison for Runs Number 1 and 2 are shown in Figures 13 and 14, respectively. These runs are for Case I, in which motion occurred only in pitch and bounce. In both runs the computer data compare closely with the field-test data in terms of both magnitude and timing. For the most part, differences are within the limits of experimental error cited above.

The comparison for Run Numbers 3, 4, and 5 are shown in Figures 13, 14, and 15, respectively. These runs are for Case II, in which one ramp was used, and motion was not restricted to pitch and bounce. In general, the comparison is almost as close as for the runs of Case I, particularly with respect to displacements (z_o, θ_{oi}, and θ_{oj}). Although the computer data compare well with the field-test data, it was of interest to analyze the data further in order to determine, if possible, the source of the differences noted.

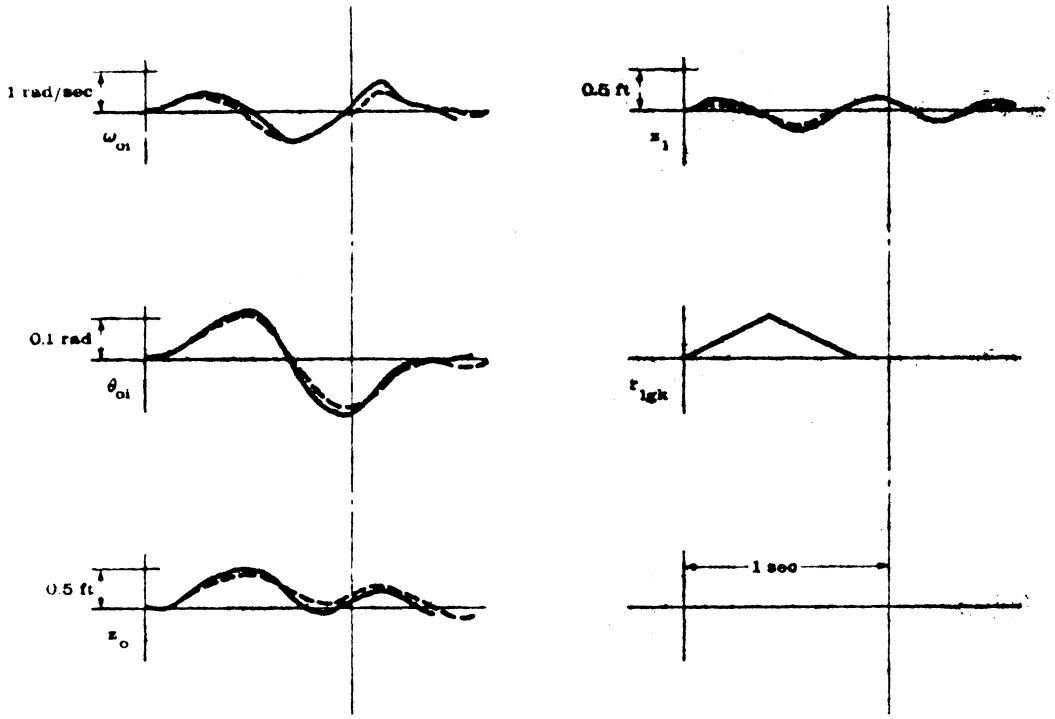

FIGURE 13. RUN NUMBER 1. Case I, 12.1 fps. —— = field test; - - - = computer.

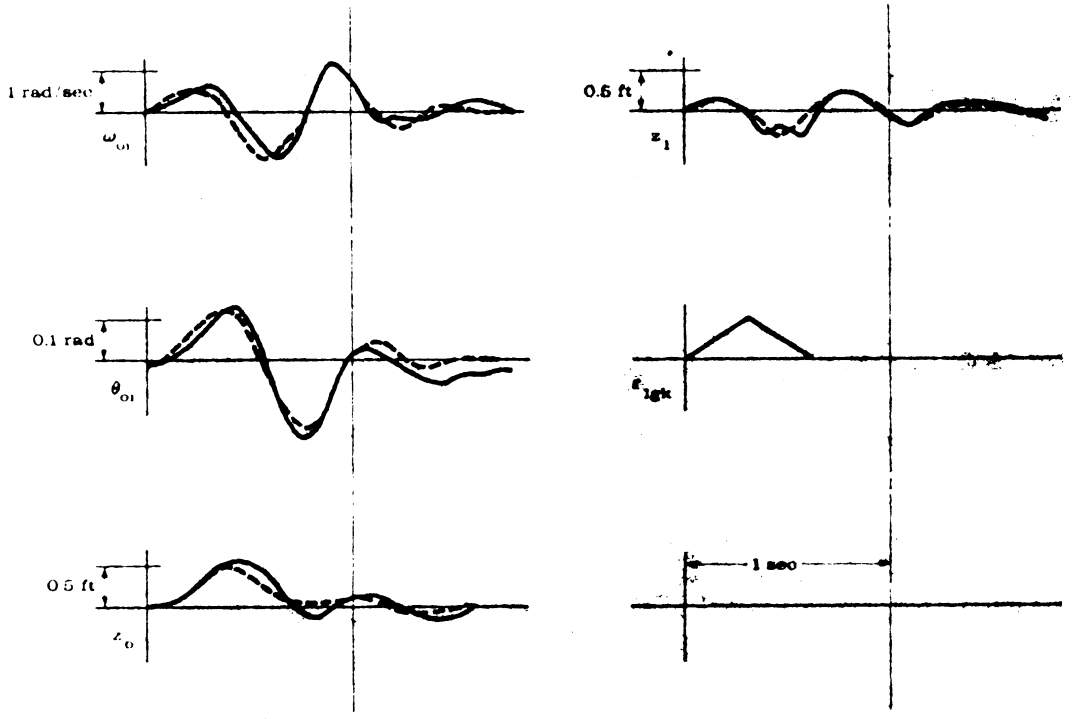

FIGURE 14. RUN NUMBER 2. Case I, 16.1 fps. —— = field test; - - - = computer.

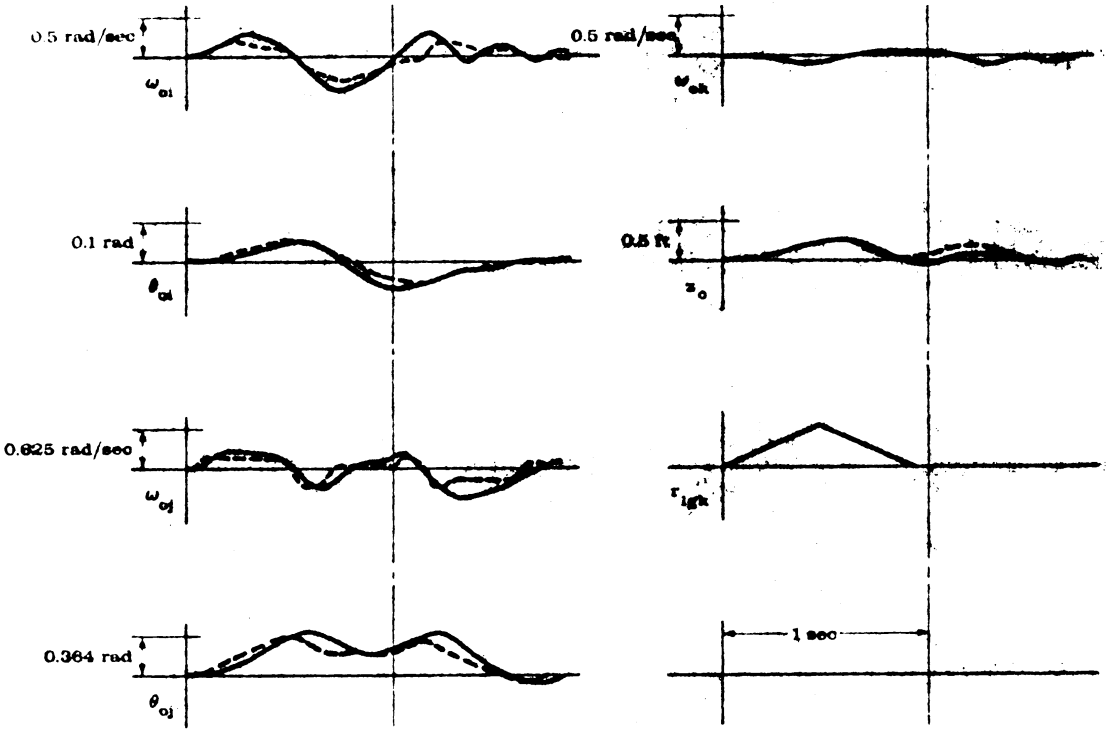

FIGURE 15. RUN NUMBER 3. Case II, 10.7 fps. —— = field test; - - - = computer.

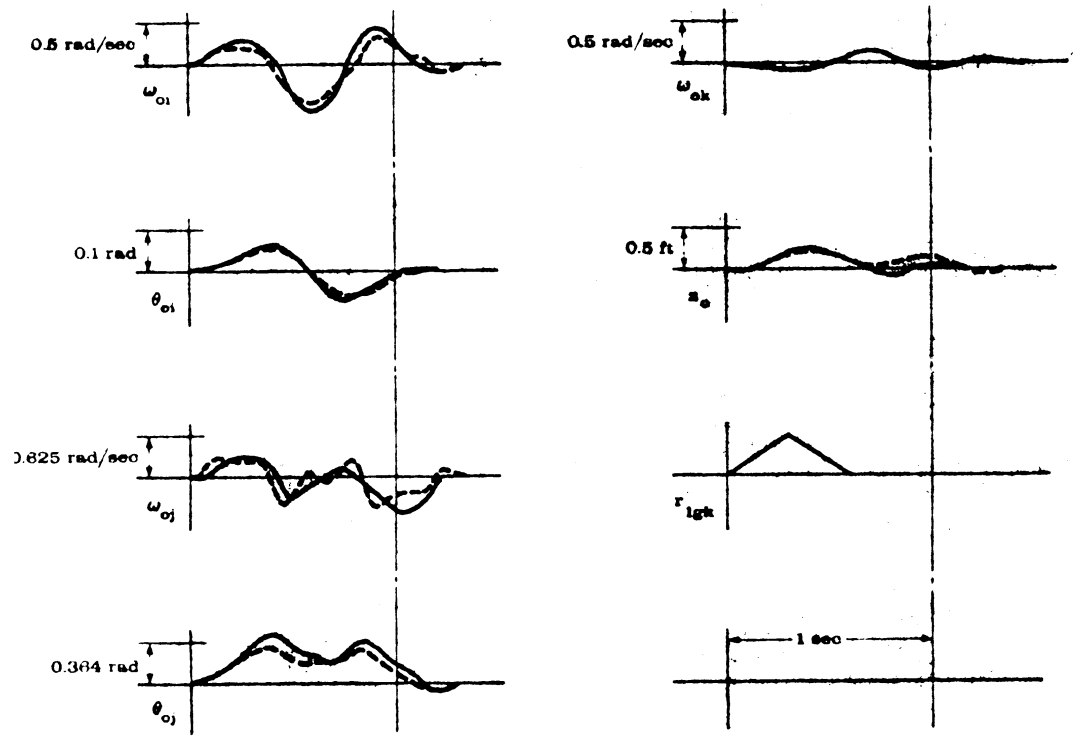

FIGURE 16. RUN NUMBER 4. Case II, 15.2 fps. —— = field test; - - - = computer.

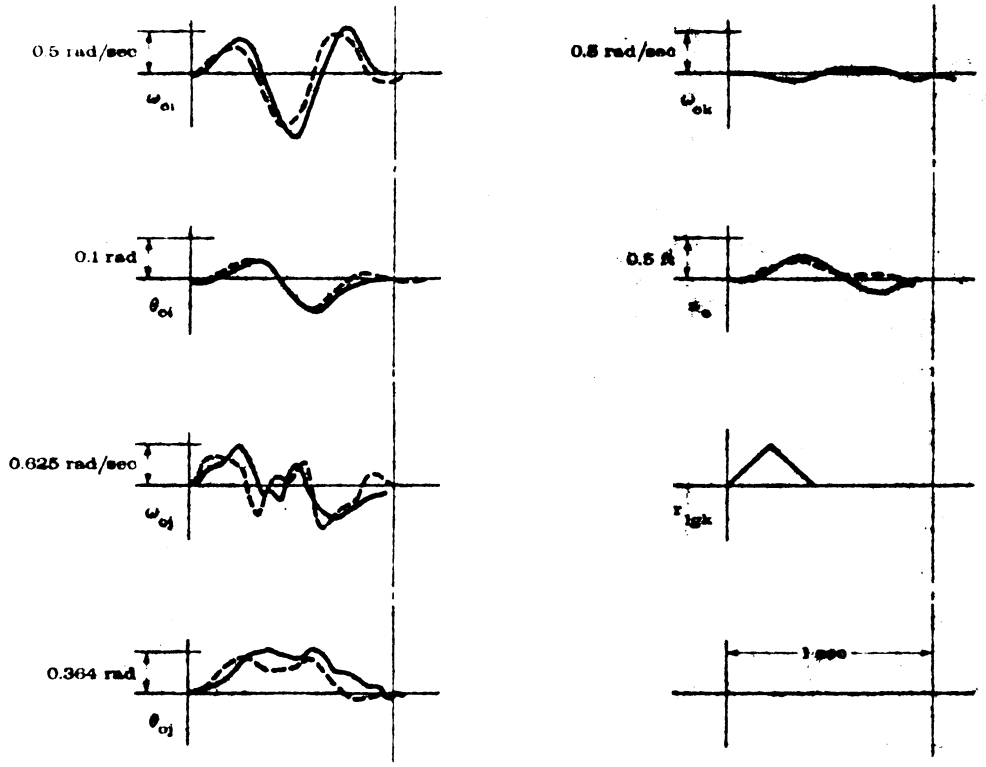

FIGURE 17. RUN NUMBER 5. Case II, 22.1 fps. —— = field test; - - - = computer.

The first step was to determine whether the differences were due to static or to dynamic inaccuracies in the equations used for the simulation. Static errors would be present in the equations if they did not correctly represent the spring characteristics or the geometry of the vehicle or the road. These errors would show up as errors in pitch and roll angles and CG height when the vehicle was standing motionless on the road. To determine whether such static errors were present, the vehicle was allowed to stand on the path over the road obstacles, while angles and distances were scaled off. It was then moved, and the measurements were repeated at 1-foot intervals. (In this case, the use of direct rather than photographic measurements increased the accuracy of the data.) This test was then simulated on the computer by running the simulation at a very low speed. The results of this test made on the vehicle for the obstacle configuration of Case II are shown in Figure 18. The computer run is not shown, because it was a nearly perfect match with the vehicle data. This demonstrates that the simulation inaccuracies are not caused by the static errors.

Figures 13, 14, and 15 indicate that there were appreciable amounts of yaw velocity (ω_{ok}) during the runs. Direct observation of the moving-picture records indicates that sideslip amounting to several inches also occurred during the Case II runs. Because of the omission of the lateral forces and accelerations in the equations used, the simulated vehicle rolls about

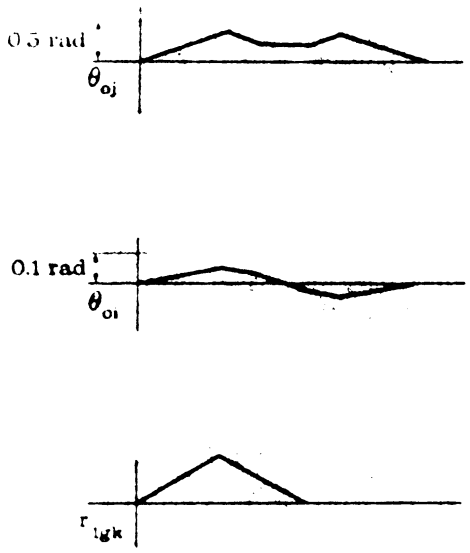

FIGURE 18. STATIC RUN. Case II obstacle configuration.

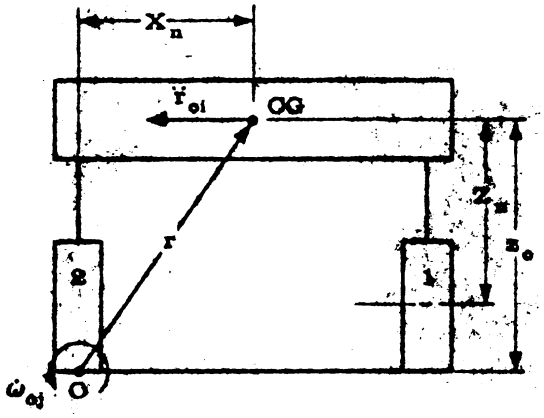

FIGURE 19. VEHICLE ROLL FOR CASE II RUN

its CG while the actual vehicle in fact rolls about some other point. In the Case II runs, for example, the vehicle wheels on one side go over the obstacle while the off-side wheels remain on level ground. Neglecting the additional effect of sideslip, the vehicle then essentially rolls about the point where the offside wheels contact the ground (Figure 19). Since the equations used for the computer simulation do not include lateral acceleration, the simulated roll will contain inaccuracies.

It is possible to allow partially for the effect of lateral motion and still utilize the simplified equations of Section B. 2 considering that this lateral motion modifies the value of roll moment of inertia which should be used in the equations. This can be done by the equation:

$$J = J_{oj} + m_o r^2$$

where r is the distance from the CG to the point about which the vehicle rolls, which is essentially fixed in the case under consideration. To check the validity of this approach, Run Number 3 was repeated on the computer with a roll moment of inertia of twice the original value, and then four times the original value (Figure 20). With a factor of 4, the computer roll data check very well with the field-test data.

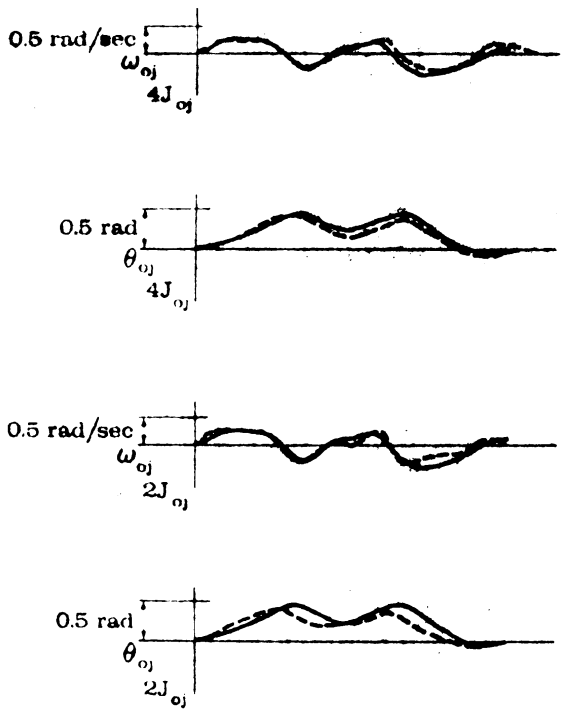

FIGURE 20. EFFECT OF INCREASED MOMENT OF INERTIA. Run Number 3. —— = field test; - - - - = computer.

If it can be shown that for a Case II run the roll equation (Equation 35b, which includes the effects of lateral motion) has the effect of increasing the roll moment of inertia by a factor of about 4, then it can be concluded that Equation 35b will accurately represent the vehicle roll for the more complicated cases (such as a Case III run) when the vehicle does not roll about a fixed point. Equation 35c, which was used in the original simulation, gave the correct roll acceleration when an increased value was used for J_{oj}, which shall be designated here as KJ_{oj}:

$$\dot{\omega}_{oj} = \frac{1}{-KJ_{oj}} \sum_n X_n F_{nk} \tag{1}$$

Substitutions will be made in Equation 35b so that it can be written in terms of KJ_{oj}. The value of K obtained from Equation 35b can then be compared with the correct value of K = 4. To begin with, the quantity z_n in Equation 35b can be ignored since it is small; this then permits the constant Z_n to be brought to the outside of the summation sign:

$$\dot{\omega}_{oj} = \frac{1}{J_{oj}} \left[Z_n \sum_n F_{ni} - \sum_n X_n F_{nk} \right] \tag{2}$$

Equation (18b) gives an expression for the term $\sum F_{ni}$:

$$\sum F_{ni} = m_o \ddot{r}_{oi} \tag{3}$$

The acceleration $\ddot{r}_{oi}$ can in turn be given by:

$$\ddot{r}_{oi} = Z_o \dot{\omega}_{oj} + X_n \omega_{oj}^2 \tag{4}$$

In this equation, the centripetal acceleration term $X_n \omega_{oj}^2$ is small compared with $Z_o \dot{\omega}_{oj}$ (see Figure 12); hence it will be ignored. Thus, if Equations 3 and 4 are used, Equation 2 can be rewritten:

$$\dot{\omega}_{oj} = \frac{1}{J_{oj}} \left[Z_n m_o z_o \dot{\omega}_{oj} - \sum_n X_n F_{nk} \right] \tag{5}$$

Now Equations 1 and 5 can be combined to eliminate the term $\sum_n X_n F_{nk}$:

$$\dot{\omega}_{oj} = \frac{1}{J_{oj}} \left[Z_n m_o z_o \dot{\omega}_{oj} + KJ_{oj} \dot{\omega}_{oj} \right] \tag{6}$$

From Equation 6, it is now possible to obtain an expression for KJ_{oj}:

$$KJ_{oj} = J_{oj} - Z_n m_o z_o . \tag{7}$$

The factor of increase to be used for J_{oj} is then:

$$K = 1 - \frac{Z_n m_o Z_o}{J_{oj}} \tag{8}$$

The values of the constants in Equation 8 are:

$Z_n = -1.46$ feet
$m_o = 59.1$ slugs
$Z_o = 2.00$ feet
$J_{oj} = 84$ lb-ft-sec^2

Using these values, in Equation 8, a value of K = 3.06 is obtained. This is not quite the factor of 4 desired. However, in computing $\ddot{r}_{oi}$ only the acceleration caused by rotation was considered and the lateral acceleration of the whole vehicle caused by sideslip was neglected. This sideslip acceleration will increase K. In the equations of Section B.1, sideslip is accounted for, so that Equation 35b will give a true representation of the vehicle roll. This substantially confirms the conclusion that the accuracy of the simulation can be improved by accounting for lateral motion.

The computer pitch data would probably more accurately match the field-test data if surge acceleration, $\ddot{r}_{oj}$, were added to the equations. However, to do this, the simplifying assumption that the vehicle has a constant forward velocity could not be used.

The comparison for Run Numbers 6 and 7 are shown in Figures 21 and 22, respectively. These runs are for Case III, in which two ramps were used on each side, and motion was not restricted to pitch and bounce. Note that, because of the presence of ramps under each wheel track, the maximum values of roll are about 0.05 rad as compared with 0.36 rad for Case II runs. The difference in scales between Case II and Case III graphs should be allowed for in considering how well the data compare. In general, the comparison is less satisfactory for Case III runs than for Case I and Case II runs.

In Run Number 6, the real and simulated data are in fairly good agreement for the first 0.6 second. After this time, the real and simulated curves diverge noticeably. Discontinuities in some of the curves at 0.65 second indicate that both the real and simulated vehicles are hitting the road on the left front wheel, but the effects on the motion are different, presumably because of differences in body position and velocity at the instant of contact.

In Run Number 7, the field-test run for roll velocity is not consistent with that for roll angle; that is, integration of the roll-velocity curve does not give the roll-angle curve. Roll-velocity data were obtained from rate-gyro measurements, whereas roll-angle data were obtained from moving-picture records. This discrepancy within the field-test data makes it difficult to arrive at conclusions regarding the run. It appears, however, that the pitch-angle data tend to follow the same trend as that for Run Number 6.

4
CONCLUSIONS and RECOMMENDATIONS

The experimental and analytical program described in this report leads to the following conclusions:

(1) A complete set of equations of vehicle motion for a wheeled vehicle has been developed and is summarized in Appendix A. These equations permit the analysis of

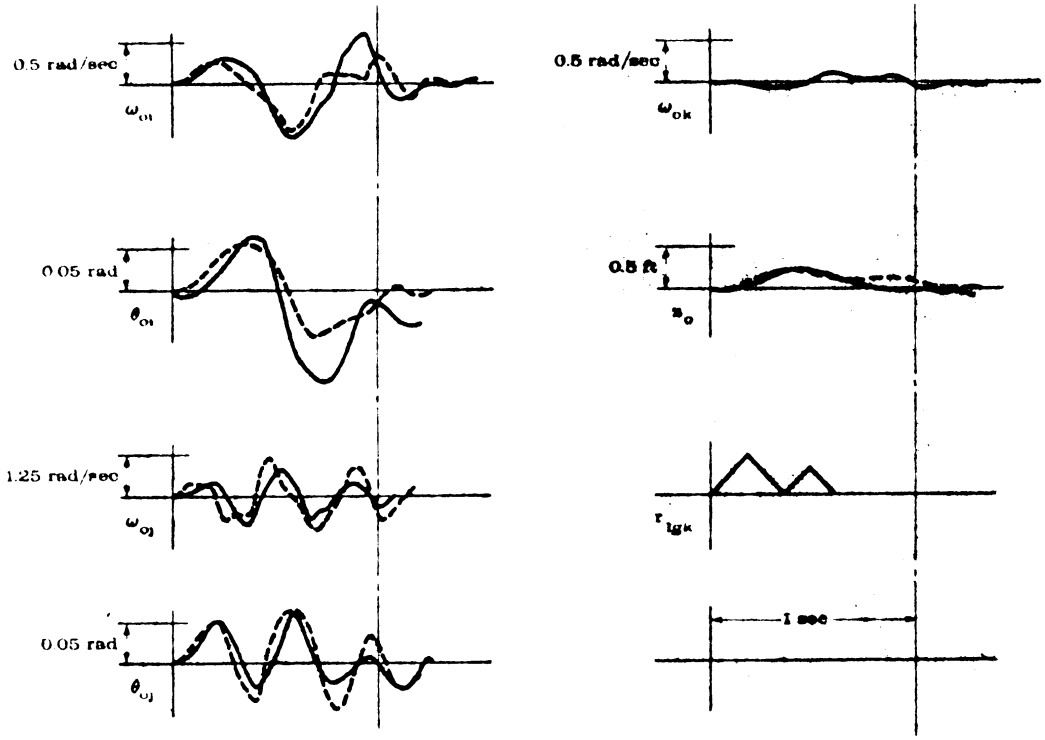

FIGURE 21. RUN NUMBER 6. Case III, 16.7 fps. —— = field test; - - - = computer.

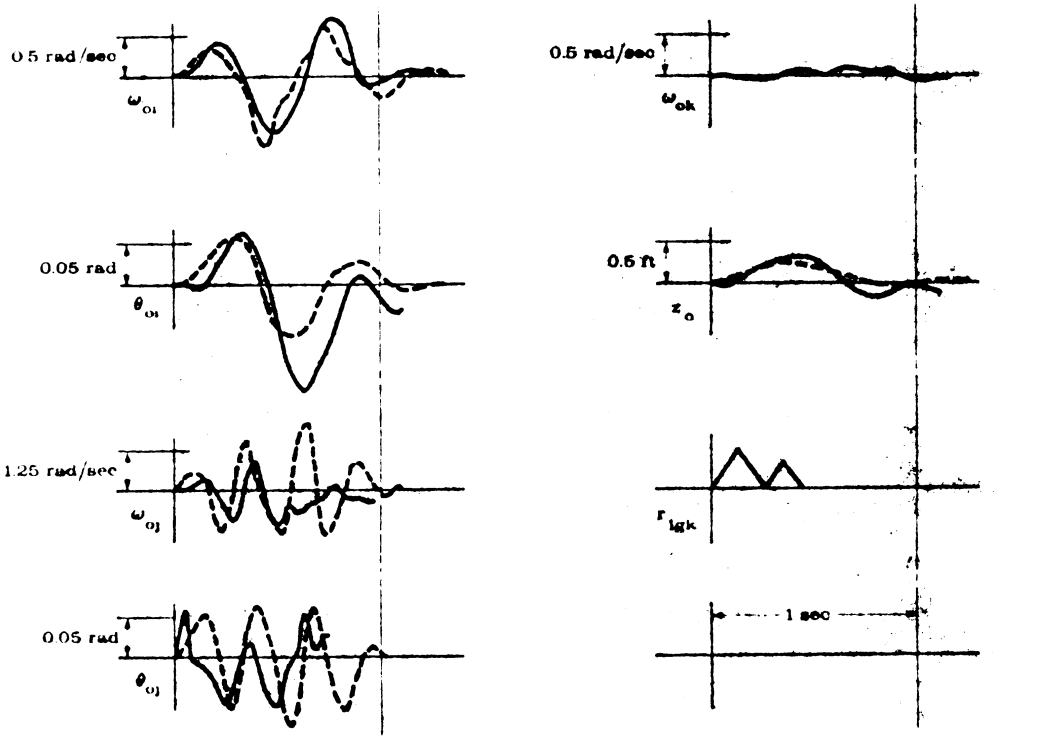

FIGURE 22. RUN NUMBER 7. Case III, 23.6 fps. —— = field test; - - - = computer.

motion in pitch, yaw, roll, bounce, surge, and sideslip. Simplifying assumptions are kept to a minimum.

(2) For many purposes, the equations of Appendix A can be reduced in complexity by making further simplifying assumptions and by restricting the number of degrees of freedom. The equations of Appendix B represent such a simplification for vehicle studies in which pitch, roll, bounce, and sideslip are represented.

(3) An experimental program involving the comparison of field-test data and the analog-computer simulation of an XM-151 military truck indicates that the equations of Section B. 2 give satisfactory results under the conditions for which they were prepared. However, the equations of Section B. 1 result in improved accuracy of computation and are recommended for use in computer studies.

(4) Further improvements in the accuracy with which vehicle motion can be simulated by computer techniques are believed to be possible. This could be accomplished by the use of improved instrumentation methods for field testing, for example, the use of magnetic tape recorders and the adaptation of gyros, accelerometers, and other measurement devices of greater accuracy and versatility. There are possibilities for simplifying the analysis of field-test data by feeding the recorded data from the magnetic tape reproducer directly into a computer setup.

(5) Additional sets of simplified equations might be developed for other restricted types of studies. The equations of Appendix A might, for example, be reduced to a two-dimensional set suitable for pitch, bounce, and surge studies. Studies of steering and handling characteristics would require the use of equations which include yaw, roll, and sideslip. For studies of this type, accurate representation of the forces induced by slipping of the tires would be required.

Appendix A
EQUATIONS of MOTION

The steps given in Section 2 for developing the complete equations of motion of a wheeled vehicle are outlined below.

(1) Equations are written representing Newton's laws of motion for both rotational and translational effects of the body and of each wheel.

(2) Relations are written which represent forces transmitted by springs, shock absorbers, and tires as functions of wheel displacement and velocity with respect to the body or to the ground.

(3) Coordinate-transformation equations are written relating displacements, velocities, and accelerations in body-fixed coordiantes to those in earth-based coordinates.

A.1. METHODS OF NOTATION

The reader should be familiar with the use of vectors to describe the position of points in space and should be familiar with the vector-product operation (Reference 3, Chapter I and IX). Appropriate sections of References 3 or 4 are cited when it is believed they would be useful. The vector product is used to describe the moments on a body, and velocities and accelerations when a moving coordinate system is involved.

The equations are written for a vehicle with a total of N wheels, individual wheels being designated by n. The summation notation, $\sum_n$, used in the equations in a condensation of the more complete notation, $\sum_{n=1}^{N}$.

To explain the subscript notation one can use as an example the position vector $\bar{r}_n$ shown in Figure 23. The bar indicates a vector quantity. The subscript n indicates that the vector quantity is associated with the n-th wheel; the subscript o indicates that it is the position vector of the body CG. The vector $\bar{r}_n$ has components in i', j', and k' directions, which are denoted as $r_{ni'}$, $r_{nj'}$, and $r_{nk'}$, respectively.

The two coordinate systems used are also shown in Figure 22. The lower-case letters, x, y, z denote coordinates in the body-fixed coordinate system, and $\bar{i}$, $\bar{j}$, and $\bar{k}$ are unit vectors in this coordinate system. The primed symbols are the corresponding quantities in the earth-based coordinate system. The capital letters X_n, Y_n, and Z_n are fixed dimensions of the vehicle. X_n is the lateral distance of the n-th wheel from the body CG, and Z_n is the distance

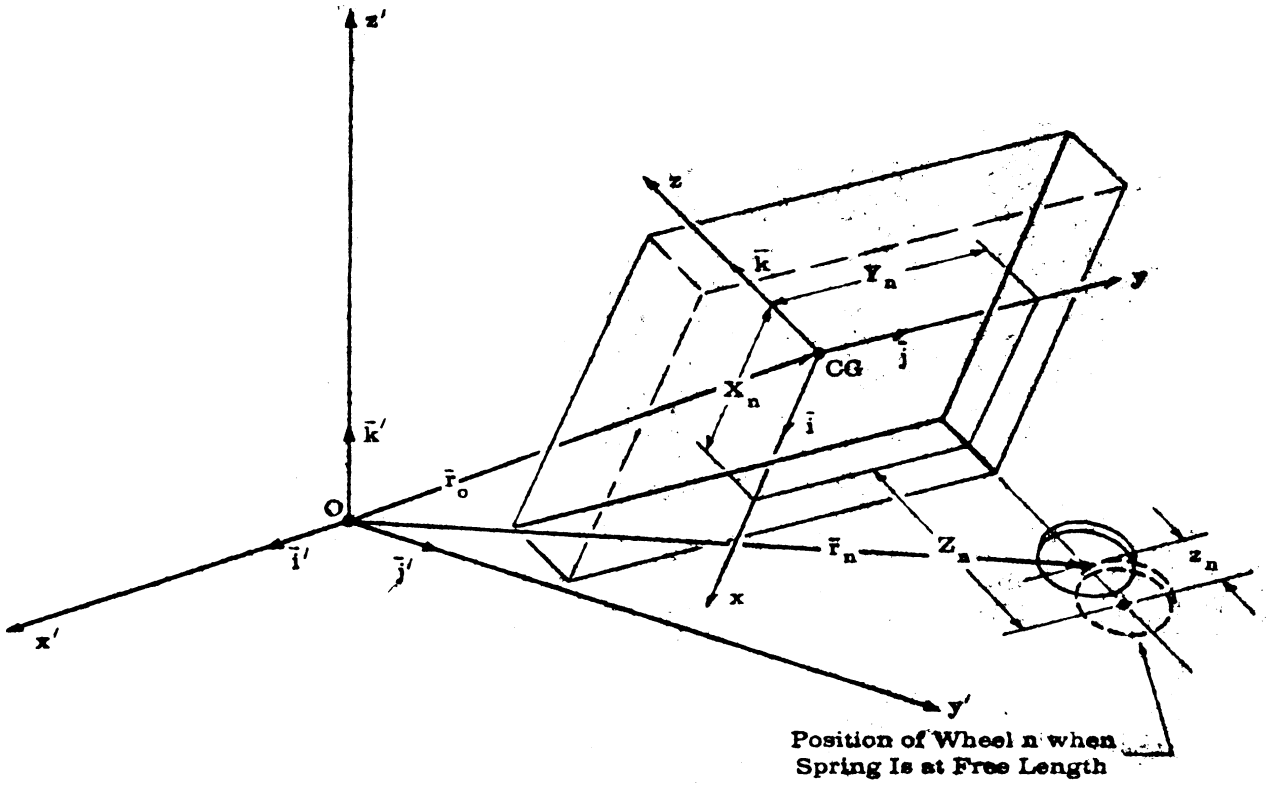

FIGURE 23. COORDINATE SYSTEMS

of the n-th wheel below the CG when the suspension spring is at its free length (i.e., in its neutral position). Since the wheels are below the CG, the Z_n are negative quantities.

The quantity z_n in Figure 22 is the distance that the n-th wheel has moved from its neutral position. In the equations developed here the wheels are constrained to move only in the z direction so that the terms x_n and y_n do not appear. If it were desired to describe the suspension in more detail, it would be necessary to write an equation in x_n, y_n, and z_n, which would define the path of the wheel as it moved with respect to the body.

A. 2. POSITION VECTORS

In this section, equations are derived relating wheel and body positions, velocities, and accelerations. The vector $\bar{r}_o$ shown in Figure 22 is the position of the body CG in the earth-based coordinate system. We have

$$\bar{r}_o = r_{oi'}\bar{i}' + r_{oj'}\bar{j}' + r_{ok'}\bar{k}' = x'_o\bar{i}' + y_{o'}\bar{j}' + z'_o\bar{k}' \tag{9}$$

Differentiating Equation 9:

$$\dot{\bar{r}}_o = \dot{x}_o\bar{i}' + \dot{y}_o\bar{j}' + \dot{z}_o\bar{k}' \tag{10}$$

and again differentiating:

$$\ddot{\bar{r}}_o = \ddot{x}_o\bar{I} + \ddot{y}_o\bar{j} + \ddot{z}_o\bar{k} \tag{11}$$

The vector $\bar{r}_n$ is the position of the n-th wheel from the origin of the earth-based system. It can be written as the sum of $\bar{r}_o$ plus the position of the wheel with respect to the body CG:

$$\bar{r}_n = \bar{r}_o + X_n\bar{i} + Y_n\bar{j} + (Z_n + z_n)\bar{k} \tag{12}$$

It should be noted that the first term on the right-hand side of Equation 12 has been given in the earth-based coordinate system by Equation 9, while the remaining terms are in the body-fixed coordinate system. If the components of $\bar{r}_n$ are desired in the body-fixed coordinates it will be necessary to apply the coordinate transformation of Section A.7 to Equation 9 to express $\bar{r}_o$ in the body-fixed coordinates. Conversely, to express $\bar{r}_n$ in earth-based coordinates, the last three terms of Equation 12 must be transformed into the earth-based coordinates.

In differentiating Equation 12, the unit vectors $\bar{i}$, $\bar{j}$, and $\bar{k}$ have derivatives since they are not constant with respect to time. The procedure for differentiating a time-varying unit vector is developed in Reference 3, Section 12.3, with the resulting equations:

$$\frac{d\bar{i}}{dt} = \bar{\omega}_o x\bar{i}$$

$$\frac{d\bar{j}}{dt} = \bar{\omega}_o x\bar{j}$$

$$\frac{d\bar{k}}{dt} = \bar{\omega}_o x\bar{k} \tag{13}$$

where $\bar{\omega}_o$ is the angular velocity vector of the body,

$$\bar{\omega}_o = \omega_{oi}\bar{i} + \omega_{oj}\bar{j} + \omega_{ok}\bar{k} \tag{14}$$

The symbol x in Equation 13 is the vector-product operation which is explained in Reference 3, Chapter IX. Differentiating Equation 12 by the use of Equations 13 and 14:

$$\ddot{\bar{r}}_n = \ddot{\bar{r}}_o + \left[\omega_{oj}(Z_n + z_n) - \omega_{ok}\dot{Y}_n\right]\bar{I} + \left[\omega_{ok}\dot{X}_n - \omega_{oi}(Z_n + z_n)\right]\bar{j} + \left[\dot{z}_n + \omega_{oi}\dot{Y}_n - \omega_{oj}\dot{X}_n\right]\bar{k} \tag{15}$$

and

$$\ddot{\bar{r}}_n = \ddot{\bar{r}}_o + \left[\dot{\omega}_{oj}(Z_n + z_n) - \dot{\omega}_{ok}Y_n + \omega_{oi}\omega_{oj}Y_n + \omega_{oi}\omega_{ok}(Z_n + z_n) - \left(\omega_{oj}^2 + \omega_{ok}^2\right)X_n + 2\omega_{oj}\dot{z}_n\right]\bar{i}$$
$$+ \left[\dot{\omega}_{ok}X_n - \dot{\omega}_{oi}(Z_n + z_n) + \omega_{oj}\omega_{ok}(Z_n + z_n) + \omega_{oi}\omega_{oj}X_n - \left(\omega_{oi}^2 + \omega_{ok}^2\right)Y_n - 2\omega_{oi}\dot{z}_n\right]\bar{j}$$
$$+ \left[\dot{\omega}_{oi}Y_n - \dot{\omega}_{oj}X_n + \omega_{oi}\omega_{ok}X_n + \omega_{oj}\omega_{ok}Y_n - \left(\omega_{oi}^2 + \omega_{oj}^2\right)(Z_n + z_n) + \ddot{z}_n\right]\bar{k} \qquad (16a)^1$$

A.3. BODY TRANSLATIONAL AND ROTATIONAL EQUATIONS

The translational and rotational motions of the body may now be derived using Newton's laws of motion as a basis. The vector equation for the body translation is

$$m_o\ddot{\bar{r}}_o = \sum_n \bar{F}_n + m_o\bar{g} \qquad (17)$$

where m_o = mass of the body

$\bar{F}_n$ = vector force acting on the body from the n-th wheel

$\bar{g}$ = gravity vector

Equation 17 in scalar form is

$$m_o\ddot{r}_{oi} = m_o\ddot{x}_o = \sum_n F_{ni} + m_o g c_{ik'} \qquad (18a)$$

$$m_o\ddot{r}_{oj} = m_o\ddot{y}_o = \sum_n F_{nj} + m_o g c_{jk'} \qquad (19a)$$

$$m_o\ddot{r}_{ok} = m_o\ddot{z}_o = \sum_n F_{nk} + m_o g c_{kk'} \qquad (20a)$$

The $c_{ik'}$ term in Equation (18a) is the direction cosine of the angle between the i and k' axes. The evaluation of the direction cosine comes directly out of the coordinate-transformation matrix which is developed in Section A.7.

The vector equation for the body rotation is

$$\frac{d\bar{H}_o}{dt} = \bar{M}_o \qquad (21)$$

where $\bar{H}_o$ = angular momentum vector

$\bar{M}_o$ = the vector of the moments acting on the body

[1] All equation numbers followed by the letter a are the final equations used in the simulation; other equations are presented only for development purposes.

In Equations 22 through 29, an expression is derived for the left-hand side of Equation 21 in terms of the moments of inertia and angular velocities of the body. Equations 30 through 33, which follow, express the right-hand side of Equation 21 in terms of the torques and forces acting on the body from the wheels. The corresponding i, j, and k components of the left-hand and right-hand sides of Equation 21 are then combined in Equations 34a through 36a to obtain the desired rotational equations.

The angular momentum can be expressed in the form

$$\bar{H}_o = \sum_q m_q(\bar{r}_q x \bar{v}_q) \tag{22}$$

where m_q = mass of the q-th particle of the body

$\bar{v}_q$ = velocity vector of the q-th particle

$\bar{r}_q$ = position vector of q-th particle from the body CG

Equation 22 is a standard definition of the angular momentum and is derived in Reference 4, Section 5.1, along with the relation

$$\bar{v}_q = \bar{\omega}_o x \bar{r}_q \tag{23}$$

Substituting Equation 23 into Equation 22:

$$\bar{H}_o = \sum_q m_q\left[\bar{r}_q x(\bar{\omega}_o x \bar{r}_q)\right] \tag{24}$$

When the triple vector-product operation indicated in the brackets is performed, Equation 24 becomes:

$$\begin{aligned}\bar{H}_o = &\left[\omega_{oi}\sum_q m_q\left(r_q^2 - x_q^2\right) - \omega_{oj}\sum_q m_q x_q y_q - \omega_{ok}\sum_q m_q x_q z_q\right]\bar{i} \\ &+\left[\omega_{oj}\sum_q m_q\left(r_q^2 - y_q^2\right) - \omega_{ok}\sum_q m_q y_q z_q - \omega_{oi}\sum_q m_q x_q y_q\right]\bar{j} \\ &+\left[\omega_{ok}\sum_q m_q\left(r_q^2 - z_q^2\right) - \omega_{oi}\sum_q m_q x_q z_q - \omega_{oj}\sum_q m_q y_q z_q\right]\bar{k}\end{aligned} \tag{25}$$

The indicated summations are merely the definitions of the moments of inertia and products of inertia.

$$\begin{aligned}J_{oi} &= \sum_q m_q\left(r_q^2 - x_q^2\right), \quad P_{oij} = \sum_q m_q x_q y_q \\ J_{oj} &= \sum_q m_q\left(r_q^2 - y_q^2\right), \quad P_{oik} = \sum_q m_q x_q z_q \\ J_{ok} &= \sum_q m_q\left(r_q^2 - z_q^2\right), \quad P_{ojk} = \sum_q m_q y_q z_q\end{aligned} \tag{26}$$

For example, the term J_{oi} is the moment of inertia of the body about the i axis and P_{oij} is the product of inertia of the body about the plane defined by the i and j axes. For most vehicles we can assume that the body is symmetrical about the (j, k) plane, giving

$$P_{oij} = P_{oik} = 0 \tag{27}$$

since for every mass particle in the positive x position there is a similar particle in the negative x direction making the corresponding summations equal to zero. Substituting Equations 26 and 27 into Equation 25:

$$\bar{H}_o = \left[J_{oi}\omega_{oi}\right]\bar{i} + \left[J_{oj}\omega_{oj} - P_{ojk}\omega_{ok}\right]\bar{j} + \left[J_{ok}\omega_{ok} - P_{ojk}\omega_{oj}\right]\bar{k} \tag{28}$$

Differentiating Equation 28 and remembering that the $\bar{i}$, $\bar{j}$, and $\bar{k}$ vectors must also be differentiated as in Equation 13, the rate of change of angular momentum is

$$\begin{aligned}\frac{d\bar{H}_o}{dt} = &\left[J_{oi}\dot{\omega}_{oi} + (J_{ok} - J_{oj})\omega_{oj}\omega_{ok} + P_{ojk}\left(\omega_{ok}^2 - \omega_{oj}^2\right)\right]\bar{i} \\ &+ \left[J_{oj}\dot{\omega}_{oj} - P_{ojk}\dot{\omega}_{ok} + (J_{oi} - J_{ok})\omega_{oi}\omega_{ok} + P_{ojk}\omega_{oi}\omega_{oj}\right]\bar{j} \\ &+ \left[J_{ok}\dot{\omega}_{ok} - P_{ojk}\dot{\omega}_{oj} + (J_{oj} - J_{oi})\omega_{oi}\omega_{oj} - P_{ojk}\omega_{oi}\omega_{ok}\right]\bar{k}\end{aligned} \tag{29}$$

The $J\dot{\omega}$ terms in Equation 29 are the ones usually associated with the change in angular momentum, and the terms involving the squares and products of ω are centrifugal and gyroscopic terms resulting from the use of a moving coordinate system.

Working now with the right-hand side of Equation 21: the vector moment acting on the body is the sum of the torques plus the sum of the moments acting on the body from the wheels. In vector form,

$$\bar{M}_o = \sum_n \bar{T}_n + \sum_n \left[(\bar{r}_n - \bar{r}_o)\times\bar{F}_n\right] \tag{30}$$

where $\bar{T}_n$ = the vector of the torque on the body from the n-th wheel. The quantity $(\bar{r}_n - \bar{r}_o)$ is the position vector of the n-th wheel from the body CG and can be obtained from Equation 12. The term $(\bar{r}_n - \bar{r}_o)\times\bar{F}_n$ is the vector representation of the moment about the body CG caused by

the force of the n-th wheel. This vector representation of a moment is developed in Reference 3, Section 10.1. Equation 30 in scalar form is

$$M_{oi} = \sum_n T_{ni} + \sum_n Y_n F_{nk} - \sum_n (Z_n + z_n) F_{nj} \tag{31}$$

$$M_{oj} = \sum_n T_{nj} + \sum_n (Z_n + z_n) F_{ni} - \sum_n X_n F_{nk} \tag{32}$$

$$M_{ok} = \sum_n T_{nk} + \sum_n X_n F_{nj} - \sum_n Y_n F_{ni} \tag{33}$$

Equating Equation 29 with Equations 31 through 33, the rotational equations for the body are

$$\sum_n T_{ni} + \sum_n Y_n F_{nk} - \sum_n (Z_n + z_n) F_{nj} = J_{oi}\dot{\omega}_{oi} + (J_{ok} - J_{oj})\omega_{oj}\omega_{ok} + P_{ojk}\left(\omega_{ok}^2 - \omega_{oj}^2\right) \tag{34a}$$

$$\sum_n T_{nj} + \sum_n (Z_n + z_n) F_{ni} - \sum_n X_n F_{nk} = J_{oj}\dot{\omega}_{oj} - P_{ojk}\dot{\omega}_{ok} + (J_{oi} - J_{ok})\omega_{oi}\omega_{ok} + P_{ojk}\omega_{oi}\omega_{oj} \tag{35a}$$

$$\sum_n T_{nk} + \sum_n X_n F_{nj} - \sum_n Y_n F_{ni} = J_{ok}\dot{\omega}_{ok} - P_{ojk}\dot{\omega}_{oj} + (J_{oj} - J_{oi})\omega_{oi}\omega_{oj} - P_{ojk}\omega_{oj}\omega_{ok} \tag{36a}$$

A.4. WHEEL TRANSLATIONAL AND ROTATIONAL EQUATIONS

The translational and rotational equations for the wheels are written in the same manner as they were for the body. The forces acting on a wheel are gravity, g; the force from the body through the suspension, F_n; and the ground-reaction force on the wheel, G_n. The translational vector equation for the n-th wheel is

$$m_n \ddot{\bar{r}}_n = \bar{G}_n - \bar{F}_n + m_n \bar{g} \tag{37}$$

and when written in scalar form it becomes:

$$m_n \ddot{r}_{ni} = G_{ni} - F_{ni} + m_n g c_{ik}, \tag{38a}$$

$$m_n \ddot{r}_{nj} = G_{nj} - F_{nj} + m_n g c_{jk}, \tag{39a}$$

$$m_n \ddot{r}_{nk} = G_{nk} - F_{nk} + m_n g c_{kk}, \tag{40a}$$

The vector equation for the n-th wheel rotation is

$$\frac{d\bar{H}_n}{dt} = \bar{M}_n \tag{41}$$

which is similar to Equation 21. By developing the right-hand side of Equation 41 in the same manner that the right-hand side of Equation 21 was developed,

$$\frac{d\bar{H}_n}{dt} = \left[J_{ni}\dot{\omega}_{ni}\right]\bar{I} + \left[J_{nj}\dot{\omega}_{oj} + (J_{ni} - J_{nk})\omega_{ni}\omega_{ok}\right]\bar{J} + \left[J_{nk}\dot{\omega}_{ok} + (J_{nj} - J_{ni})\omega_{ni}\omega_{oj}\right]\bar{k} \qquad (42)$$

Several substitutions have been made in Equation 42. It has been assumed that the wheel is a disc so that the products of inertia are equal to zero:

$$P_{nij} = P_{nik} = P_{njk} = 0 \quad \text{and} \quad J_{nj} = J_{nk}$$

Also, since the wheels rotate with the body about the j and k axes,

$$\omega_{nj} = \omega_{oj} \quad \text{and} \quad \omega_{nk} = \omega_{ok}$$

The suspension, connecting the wheel to the body, is neither wholly a part of the wheel nor of the body. A true representation of the suspension would lead to a system with distributed parameters. A good approximation for a conventional suspension is to lump one-third of its mass with the body and two-thirds with the wheel. As a further approximation, the wheel is assumed to be a disk in the model used here. This lends simplicity to the equations and is not considered to produce noticeable errors in the simulation, particularly when the wheel mass is large compared to that of the suspension.

The moment equation for the n-th wheel is developed in a manner similar to that for Equation 30 for the body:

$$\bar{M}_n = -\bar{T}_n + \bar{r}_{nw} x \bar{G}_n \qquad (43)$$

The vector $\bar{r}_{nw}$, shown in Figure 24, is the vector from the wheel center to the ground-contact point so that the term $\bar{r}_{nw} x \bar{G}_n$ gives the moment around the wheel center caused by the ground-reaction force, $\bar{G}_n$. In the mathematical model developed here it is assumed that the tire contacts the ground at a point which lies on the k axis when this axis is extended through the wheel center (Figure 24). Since the vector $\bar{r}_{nw}$ has a component only in the k direction, it can be written

$$\bar{r}_{nw} = r_{rw}\bar{k} \qquad (44)$$

For the purposes of Equation 43, one can make the further simplification that

$$r_{nw} = -R_w \qquad (45)$$

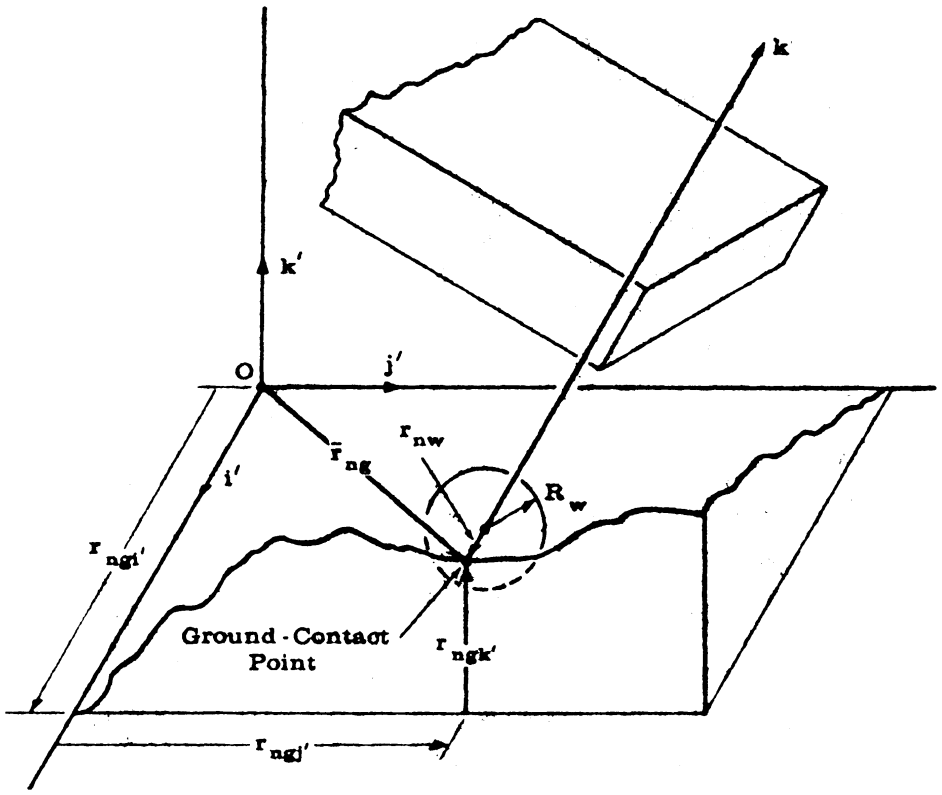

FIGURE 24. SYMBOLS FOR THE WHEEL AND THE GROUND

The quantity R_w (Figure 24) is the radius of the wheel, including the tire. The minus sign appears in Equation 45 because r_{nw} is defined as the distance from the wheel center down to the ground-contact point, a negative quantity, whereas R_w is a radius, which is a positive quantity. Substituting Equations 44 and 45 into Equation 43 and writing in scalar form:

$$M_{ni} = -T_{ni} + R_w G_{nj} \tag{46}$$

$$M_{nj} = -T_{nj} - R_w G_{ni} \tag{47}$$

$$M_{nk} = -T_{nk} \tag{48}$$

Equating Equation 42 with Equations 46 through 48,

$$-T_{ni} + R_w G_{nj} = J_{ni}\dot{\omega}_{ni} \tag{49a}$$

$$-T_{nj} - R_w G_{ni} = J_{nj}\dot{\omega}_{oj} + (J_{ni} - J_{nk})\omega_{ni}\omega_{ok} \tag{50a}$$

$$-T_{nk} = J_{nk}\dot{\omega}_{ok} + (J_{nj} - J_{ni})\omega_{ni}\omega_{oj} \tag{51a}$$

The torque T_{ni} consists mainly of the driving, braking, and bearing friction torques applied to the wheel.

An equation can be written for the wheel angular velocity, ω_{ni}, if it is assumed that the wheel rolls along the ground without slipping. Neglecting the effect of rotations of the body about the i axis, the angular velocity of the wheel is the linear velocity of the wheel center, $\dot{r}_{nj}$, divided by the distance from the wheel center to the ground-contact point:

$$\omega_{ni} = \frac{\dot{r}_{nj}}{r_{nw}} \tag{52}$$

Differentiating Equation 52:

$$\dot{\omega}_{ni} = \frac{r_{nw}\ddot{r}_{nj} - \dot{r}_{nw}\dot{r}_{nj}}{r_{nw}^2} \tag{53a}$$

A. 5. GROUND-CONTACT POINT

In order to develop equations for the ground-reaction forces, it is necessary to write equations which describe the point at which the tire contacts the ground. As shown in Figure 24, the vector $\bar{r}_{ng}$ is the position vector of the ground-contact point with respect to the origin of the earth-based coordinate system. It can be seen that

$$\bar{r}_{ng} = \bar{r}_n + \bar{r}_{nw} \tag{54}$$

An expression for the wheel position vector, $\bar{r}_n$, is given by Equation 12, and $\bar{r}_{nw}$ is given by Equation 44. Considering the i' component of Equation 54,

$$r_{ngi'} = r_{ni'} + r_{nw}c_{ki'} \tag{55a}$$

Similarly, for the j' component,

$$r_{ngj'} = r_{nj'} + r_{nw}c_{kj'} \tag{56a}$$

Because the vehicle can travel in the three dimensions, the ground over which the vehicle travels must be described by a surface, as shown in Figure 24. The equation for a surface is of the form

$$z = f(x, y) \tag{57}$$

Equations 55a and 56a are expressions for the x and y of Equation 57, so that the elevation of the ground at the wheel contact point is given by

$$r_{ngk'} = f(r_{ngi'}, r_{ngj'}) \tag{58a}$$

which can be determined by a survey of the land over which the vehicle travels. If the vehicle is to travel over a prescribed path, Equation 57 reduces to a two-dimensional equation of the form

$$z = f(x)$$

To have a complete set of equations, it is necessary to write an equation which expresses r_{nw} in terms of previously defined quantities. From the geometry of Figure 24, it can be seen that

$$r_{nw} = \frac{r_{ngk'} - r_{nk'}}{c_{kk'}} \tag{59a}$$

A.6. FORCE EQUATIONS

The equations previously derived have included terms representing the various forces acting on the vehicle. These forces can be described in terms of wheel displacement and velocity with respect to the body or the ground. The force F_{nk} is the force on the body or wheel caused by the suspension spring and shock absorber:

$$F_{nk} = K_{ns}(z_n) + C_{ns}(\dot{z}_n)\phi_{ns}(z_n) \tag{60a}$$

The first term on the right-hand side of Equation 60a is the force on the body caused by the suspension spring. It is the spring force-vs.-displacement function which has the spring displacement z_n as the independent variable. The function $C_{ns}(\dot{z}_n)$ is the suspension shock-absorber force-vs.-velocity characteristic. The shock-absorber force may depend not only on its velocity but also on displacement; hence the term $\phi_{ns}(z_n)$.

The tire exhibits spring and damping characteristics in much the same manner as the suspension. Thus,

$$G_{nk} = K_{nw}(R_w + r_{nw}) + C_{nw}(\dot{r}_{nw})\phi_{nw}(R_w + r_{nw}) \tag{61a}$$

The independent variable $(R_w + r_{nw})$ and its derivative $(\dot{r}_{nw})$ are, respectively, the amount the tire is deflected (Figure 24), and its deflection rate.

Expressions will now be derived for G_{ni}, the sideward force exerted on the wheel by the ground. Two conditions will be considered, one in which the tire does not slip sidewise, the other in which it does.

The vector $\bar{r}_{ng}$ is the position vector of the ground-contact point from the origin of the earth-based coordinate system. The i component of the corresponding acceleration vector, $\ddot{r}_{ngi}$, will be derived as a function of forces acting on the wheel. From Figure 24,

$$\bar{r}_{ng} = \bar{r}_n + \bar{r}_{nw} = \bar{r}_n + r_{nw}\bar{k} \tag{62}$$

Differentiating this equation gives

$$\dot{\bar{r}}_{ng} = \dot{\bar{r}}_n + \dot{r}_{nw}\bar{k} + r_{nw}\frac{d\bar{k}}{dt} \tag{63}$$

and since

$$\frac{d\bar{k}}{dt} = \bar{\omega}_o \times \bar{k} \tag{13}$$

then

$$\dot{\bar{r}}_{ng} = \dot{\bar{r}}_n + \dot{r}_{nw}\bar{k} + r_{nw}(\bar{\omega}_o \times \bar{k}) \tag{64}$$

Differentiating Equation 64, multiplying both sides by m_n, and taking the i component:

$$m_n \ddot{r}_{ngi} = m_n \ddot{r}_{ni} + m_n(\dot{\omega}_{oj} r_{nk} + \omega_{oi}\omega_{ok} r_{nk} + 2\omega_{oj}\dot{r}_{nk}) \tag{65}$$

Substituting for $m_n \ddot{r}_{ni}$ from Equation 38:

$$m_n \ddot{r}_{ngi} = G_{ni} - F_{ni} + m_n g c_{ik'} + m_n(\dot{\omega}_{oj} r_{nk} + \omega_{oi}\omega_{ok} r_{nk} + 2\omega_{oj}\dot{r}_{nk}) \tag{66}$$

Two cases may be distinguished. In Case 1, $|G_{ni}|$ remains less than $|\mu G_{nk}|$, where μ is the coefficient of friction and G_{nk} is the k component of ground reaction. Under this condition, the wheel will not slip sidewise. For Case 1, the following conditions apply:

$$|G_{ni}| < |\mu G_{nk}| \tag{67}$$

and

$$\dot{r}_{ngi} = \ddot{r}_{gni} = 0 \tag{68}$$

so that Equation 66 becomes

$$G_{ni} = F_{ni} - m_n(g c_{ik'} + \dot{\omega}_{oj} r_{nk} + \omega_{oi}\omega_{ok} r_{nk} + 2\omega_{oj}\dot{r}_{nk}) \qquad \text{(Case 1: 69a)}$$

For Case 2, the wheel may slip sideways. Under this condition, assuming that the plane of the ground at the ground-contact point is normal to the k axis, the sideward ground-reaction force is equal to the vertical ground-reaction force times the coefficient of friction. Expressed in equation form,

$$\dot{r}_{ngi} \neq 0$$

and

$$|G_{ni}| = |\mu G_{nk}| \qquad \text{(Case 2: 70a)}$$

To compute G_{ni}, then, Equation 69a is used when the condition of Equation 67 applies. When $|G_{ni}|$ from Equation 69a becomes greater than $|\mu G_{nk}^{\cdot}|$, the magnitude of G_{ni} is given by Equation 70a. The sign of G_{ni} for the condition of Case 2 is the same as that given by Equation 69a, since G_{ni} cannot change sign without going through zero under Case 1 conditions.

It has been assumed either that there is no slideslip of the wheel or that, if there is sideslip, the coefficient of friction μ is a constant. It should be recognized that these assumptions are approximate only. In steering and handling studies a more detailed analysis would be required, one which uses either an analytical or empirical representation of the tire-slip angle.

A.7. COORDINATE TRANSFORMATION

In the preceding equations, vectors have been given in terms of one of two different coordinate systems. It is necessary to be able to convert a vector given in one set of coordinates to its representation in the other set. For example, $\bar{r}_o$ is expressed by Equation 9 in the earth-fixed coordinate system; expressed in the body-fixed coordinates:

$$\begin{aligned}\bar{r}_o = &\left[x_o c_{i'i} + y_o c_{j'i} + z_o c_{k'i}\right]\bar{i} \\ &+ \left[x_o c_{i'j} + y_o c_{j'j} + z_o c_{k'j}\right]\bar{j} \\ &+ \left[x_o c_{i'k} + y_o c_{j'k} + z_o c_{k'k}\right]\bar{k}\end{aligned} \tag{71a}$$

where the c's are the direction cosines between the axes indicated in the subscript. The direction cosines are obtained through the use of Euler angles, a method which is thoroughly discussed in Reference 4, Sections 4.1-4.4.

The Euler angles used here are Azimuth A, Elevation E, and Bank B, as shown in Figure 25. The resulting transformation matrix is:

$$[T] = \begin{bmatrix} \cos A \cos B - \sin A \sin E \sin B & \cos A \sin E \sin B + \sin A \cos B & -\cos E \sin B \sin E \\ -\sin A \cos E & \cos A \cos E & \\ \cos A \sin B + \sin A \sin E \cos B & \cos A \sin E \cos B - \sin A \sin B & \cos E \cos B \end{bmatrix} \tag{72a}$$

and

$$\begin{bmatrix} i \\ j \\ k \end{bmatrix} = \begin{bmatrix} \\ T \\ \\ \end{bmatrix} \begin{bmatrix} i' \\ j' \\ k' \end{bmatrix} \tag{73a}$$

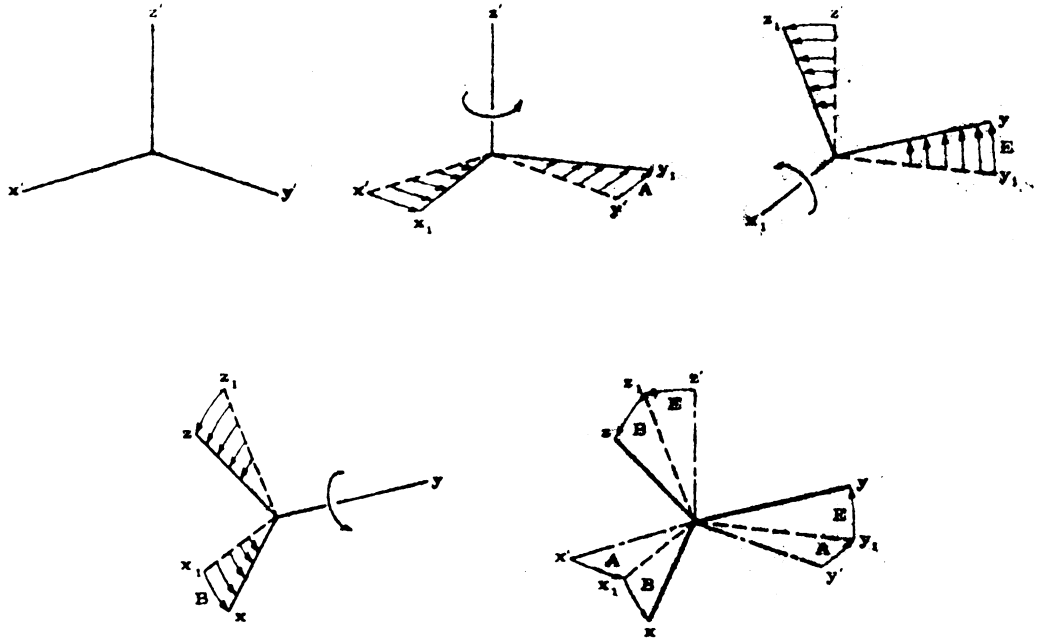

FIGURE 25. EULER ANGLES

Each of the elements of the matrix of Equation 72a is a direction cosine between an axis of one coordinate system and an axis of the other. For example, the upper left-hand element is the direction cosine between the i and i' axes, namely $c_{ii'}$. The complete transformation matrix may therefore be represented as

$$\begin{bmatrix} c_{ii'} & c_{ij'} & c_{ik'} \\ c_{ji'} & c_{jj'} & c_{jk'} \\ c_{ki'} & c_{kj'} & c_{kk'} \end{bmatrix}$$

The rates of change of the Euler angles with respect to time are given by the following:

$$\begin{aligned} \dot{A} &= \omega_{oi} c_{ik'} + \omega_{oj} c_{jk'} + \omega_{ok} c_{kk'} \\ \dot{E} &= \omega_{oi} \cos B \qquad + \omega_{ok} \sin B \\ \dot{B} &= \qquad\qquad \omega_{oj} \end{aligned} \tag{74a}$$

and the Euler angles are:

$$A = \int \dot{A}\,dt$$
$$E = \int \dot{E}\,dt \qquad (75a)$$
$$B = \int \dot{B}\,dt$$

A. 8. SIMULATION EQUATIONS

The equations to be used in the simulation (the equations with numbers followed by the letter a) are rewritten here as explicit expressions in the dependent variable.

$$\dot{\omega}_{oi} = \frac{1}{J_{oi}}\left[\sum_n T_{ni} + \sum_n Y_n F_{nk} - \sum_n (Z_n + z_n)F_{nj} + P_{oik}\dot{\omega}_{ok} - (J_{ok} - J_{oj})\omega_{oj}\omega_{ok} + P_{oik}\omega_{oi}\omega_{oj}\right] \qquad (34a)$$

$$\dot{\omega}_{oj} = \frac{1}{J_{oj}}\left[\sum_n T_{nj} + \sum_n (Z_n + z_n)F_{ni} - \sum_n X_n F_{nk} - (J_{oi} - J_{ok})\omega_{oi}\omega_{ok} - \left(\omega_{oi}^2 - \omega_{ok}^2\right)P_{oik}\right] \qquad (35a)$$

$$\dot{\omega}_{ok} = \frac{1}{J_{ok}}\left[\sum_n T_{nk} + \sum_n X_n F_{nj} - \sum_n Y_n F_{ni} + P_{oik}\dot{\omega}_{oi} - (J_{oj} - J_{oi})\omega_{oi}\omega_{oj}\right] \qquad (36a)$$

$$\ddot{x}_o = \frac{1}{m_o}\left(\sum_n F_{ni} + m_o g c_{ik'}\right) \qquad (18a)$$

$$\ddot{y}_o = \frac{1}{m_o}\left(\sum_n F_{nj} + m_o g c_{jk'}\right) \qquad (19a)$$

$$\ddot{z}_o = \frac{1}{m_o}\left(\sum_n F_{nk} + m_o g c_{kk'}\right) \qquad (20a)$$

$$\ddot{z}_n = \ddot{r}_{nk} - \ddot{r}_{ok} - \omega_{oi}(Y_n - \omega_{ok}X_n) + \omega_{oj}(X_n - \omega_{ok}Y_n) + \left(\omega_{oi}^2 + \omega_{oj}^2\right)(Z_n + z_n) \qquad \text{(k component of 16a)}$$

$$\ddot{r}_{nk} = \frac{1}{m_n}(G_{nk} - F_{nk} + m_n g c_{kk'}) \qquad (40a)$$

$$F_{nk} = K_{ns}(z_n) + C_{ns}(\dot{z}_n)\phi_{ns}(z_n) \qquad (60a)$$

$$r_{ngi'} = r_{ni'} + r_{nw}c_{ki'} \tag{55a}$$

$$r_{ngj'} = r_{nj'} + r_{nw}c_{kj'} \tag{56a}$$

$$r_{ngk'} = f(r_{ngi''}\ r_{ngj'}) \tag{58a}$$

$$r_{nw} = \frac{r_{ngk'} - r_{nk'}}{c_{kk'}} \tag{59a}$$

$$G_{nk} = K_{nw}(R_w + r_{nw}) + C_{nw}(\dot{r}_{nw})\phi_{nw}(R_w + r_{nw}) \tag{61a}$$

$$T_{nk} = -J_{nk}\dot{\omega}_{ok} - (J_{nj} - J_{ni})\omega_{ni}\omega_{oj} \tag{51a}$$

$$\dot{\omega}_{ni} = \frac{r_{nw}\ddot{r}_{nj} - \dot{r}_{nw}\dot{r}_{nj}}{r_{nw}^2} \tag{53a}$$

$$G_{nj} = \frac{J_{ni}\dot{\omega}_{ni} + T_{ni}}{R_w} \tag{49a}$$

$$\ddot{r}_{nj} = \ddot{y}_o + \dot{\omega}_{ok}X_n - \dot{\omega}_{oi}(Z_n + z_n) + \omega_{oj}\omega_{ok}(Z_n + z_n) + \omega_{oi}\omega_{oj}X_n - \left(\omega_{oi}^2 + \omega_{ok}^2\right)Y_n - 2\omega_{oi}\dot{z}_n \tag{j component of 16a}$$

$$F_{nj} = G_{nj} + m_n(gc_{jk'} - \ddot{r}_{nj}) \tag{39a}$$

$$T_{nj} = J_{nj}\dot{\omega}_{oj} - (J_{oi} - J_{ok})\omega_{ni}\omega_{ok} + R_w G_{nj} \tag{50a}$$

$$\ddot{r}_{ni} = x_o + \dot{\omega}_{oj}(Z_n + z_n) - \dot{\omega}_{ok}Y_n + \omega_{oi}\omega_{oj}Y_n \tag{i component of 16a}$$

$$F_{ni} = G_{ni} + m_n(gc_{ik'} - \ddot{r}_{ni}) \tag{38a}$$

$$G_{ni} = F_{ni} - m_n(gc_{ik'} + \dot{\omega}_{oj} r_{nk} + \omega_{oi}\omega_{ok} r_{nk} + 2\omega_{oj} \dot{r}_{nk}) \qquad \text{(Case 1: 69a)}$$

$$|G_{ni}| = |\mu G_{nk}| \qquad \text{(Case 2: 70a)}$$

$$\begin{aligned} x'_o &= x_o c_{ii'} + y_o c_{ji'} + z_o c_{ki'} \\ y'_o &= x_o c_{ij'} + y_o c_{jj'} + z_o c_{kj'} \\ z'_o &= x_o c_{ik'} + y_o c_{jk'} + z_o c_{kk'} \end{aligned} \qquad \text{(71a)}$$

$$[T] = \begin{bmatrix} \cos A \cos B - \sin A \sin E \sin B & \cos A \sin E \sin B + \sin A \cos B & -\cos E \sin B \sin E \\ -\sin A \cos E & \cos A \cos E & \\ \cos A \sin B + \sin A \sin E \cos B & \cos A \sin E \cos B - \sin A \sin B & \cos E \cos B \end{bmatrix} \qquad \text{(72a)}$$

$$\begin{bmatrix} i \\ j \\ k \end{bmatrix} = \begin{bmatrix} T \end{bmatrix} \begin{bmatrix} i' \\ j' \\ k' \end{bmatrix} \qquad \text{(73a)}$$

$$\begin{aligned} \dot{A} &= \omega_{oi} c_{ik'} + \omega_{oj} c_{jk'} + \omega_{ok} c_{kk'} \\ \dot{E} &= \omega_{oi} \cos B + \omega_{ok} \sin B \\ \dot{B} &= \omega_{oj} \end{aligned} \qquad \text{(74a)}$$

$$\begin{aligned} A &= \int \dot{A}\, dt \\ E &= \int \dot{E}\, dt \\ B &= \int \dot{B}\, dt \end{aligned} \qquad \text{(75a)}$$

Appendix B
SIMPLIFIED EQUATIONS of MOTION

The equations of Appendix A were derived in a straightforward manner from a mathematical model of the vehicle. For many applications, the equations of Appendix A can be simplified without noticeable degradation of results. In Section B.1, the equations of Appendix A are re-written using several simplifying assumptions. These equations should be sufficiently accurate

to simulate a vehicle which is not being turned through large angles and which is moving at constant speed over cross-country terrain which is not excessively rugged.

In Section B. 2, additional simplifications are made to the equations of Section B. 1 by eliminating the factors of sideslip forces and motion to derive the equations that were used to perform the analog-computer simulation of the XM-151. It was shown in Section 3. 8, when the XM-151 field-test results were compared with the simulated results, that a better simulation could be obtained if lateral motion factors were added to the equations used.

B. 1. RECOMMENDED EQUATIONS

The equations of Section A. 8 are rewritten to include the following assumptions:

(1) Since the vehicle does not roll, pitch, or yaw more than about 10°, the components of a vector are almost the same in both coordinate systems. Using a two-dimensional example: a force of magnitude F in the k direction has components in the j' and k' deviations of:

$$F\bar{k} = F \sin\theta \bar{j}' + F \cos\theta \bar{k} \simeq F\bar{k}'$$

This concept can be used to simplify the equations of Appendix A, and the coordinate transformation matrix, Equation 72a, can be written:

$$[T] = \begin{bmatrix} 1 & 0 & 0 \\ 0 & 1 & 0 \\ 0 & 0 & 1 \end{bmatrix}$$

The equations in Appendix B are written with unprimed coordinates because there is no longer a distinction between the primed and unprimed coordinates.

(2) Figure 11 shows that in the field tests the vehicle had a nearly constant forward velocity. Therefore, it is assumed here that the vehicle's forward velocity is constant:

$$r_{oj} = V$$

This implies that the forces in the forward direction acting on the vehicle are zero:

$$G_{nj} = F_{nj} = 0$$

(3) It is assumed that the torques caused by the angular accelerations of the wheels are small:

$$T_{ni} = T_{nj} = T_{nk} \simeq 0$$

Part of the torque, T_{ni}, is the driving torque, which is zero from the conditions of the preceding assumption.

(4) The products and squares of the angular velocities are assumed to be negligibly small compared with the angular accelerations. Also, it is assumed that the Coriolis' accelerations are small. Expressed mathematically,

$$\omega\omega,\ \omega^2,\ 2\omega\dot{z}_n \ll \dot{\omega}$$

Figure 12 shows the relative magnitude of some of these terms as obtained from the computer simulation discussed in Section 3.2. Since the results of any simulation will give the angular velocities, ω, and angular rates, $\dot{\omega}$, it is a simple matter to check the approximate magnitudes of the ω^2 and $\omega\omega$ terms to see whether appreciable error can occur by neglecting them in the simulation.

(5) All products of inertia are assumed to be zero.

The equations of Section A.8 are rewritten here with the above assumptions having been made. To distinguish this set of equations the letter a in the equation number has been replaced by the letter b.

$$\dot{\omega}_{oi} = \frac{1}{J_{oi}} \sum_n Y_n F_{nk} \tag{34b}$$

$$\dot{\omega}_{oj} = \frac{1}{J_{oj}} \left[\sum_n (Z_n + z_n) F_{ni} - \sum_n X_n F_{nk} \right] \tag{35b}$$

$$\dot{\omega}_{ok} = \frac{-1}{J_{ok}} \sum_n Y_n F_{ni} \tag{36b}$$

$$\ddot{r}_{oi} = \ddot{x}_o = \frac{1}{m_o} \sum_n F_{ni} \tag{18b}$$

$$\ddot{r}_{ok} = \ddot{z}_o = \frac{1}{m_o} \left[\sum_n F_{nk} + m_o g \right] \tag{20b}$$

$$\ddot{z}_n = \ddot{r}_{nk} - \ddot{z}_o - \dot{\omega}_{oi} Y_n + \dot{\omega}_{oj} X_N \qquad \text{(k component of 16b)}$$

$$\ddot{r}_{nk} = \frac{1}{m_n} \left[G_{nk} - F_{nk} + m_n g \right] \tag{40b}$$

$$F_{nk} = K_{ns}(z_n) + C_{ns}(\dot{z}_n)\phi_{ns}(z_n) \tag{60b}$$

$$r_{ngk} = f\left(t + \frac{Y_n}{V}\right) \tag{58b}$$

$$r_{nw} = r_{ngk} - r_{nk} \tag{59b}$$

$$G_{nk} = K_{nw}(R_w + r_{nw}) + C_{nw}(\dot{r}_{nw})\phi_{nw}(R_w + r_{nw}) \tag{61b}$$

$$\ddot{r}_{ni} = \ddot{x}_o + \omega_{oj}(Z_n + z_n) - \dot{\omega}_{ok}Y_n \qquad \text{(i component of 16b)}$$

$$F_{ni} = G_{ni} - m_n\ddot{r}_{ni} \tag{38b}$$

$$G_{ni} = F_{ni} - m_n\dot{\omega}_{oj}r_{nk} \qquad \text{(Case 1: 69b)}$$

$$|G_{ni}| = |\mu G_{nk}| \qquad \text{(Case 2: 70b)}$$

B. 2. EQUATIONS USED FOR COMPARISON TESTING

The equations used for the analog-computer simulation of the XM-151 (Section 3. 2) can be obtained from the equations of Section B. 1 if lateral forces and acceleration are dropped out, that is, if

$$F_{ni} = G_{ni} = \ddot{r}_{ni} = 0$$

Under these conditions the vehicle yaw, Equation 36b, also drops out, leaving only pitch, bounce, and roll. The letter c is used in the equation numbers below to distinguish this particular set. As a guide, a brief description is given for each equation.

Body Pitch

$$\dot{\omega}_{oi} = \frac{1}{J_{oi}}\sum_n Y_n F_{nk} \tag{34c}$$

Body Roll

$$\dot{\omega}_{oj} = \frac{-1}{J_{oj}}\sum_n X_n F_{nk} \tag{35c}$$

Body Bounce

$$\ddot{z}_o = \frac{1}{m_o}\left[\sum_n F_{nk} + m_o g\right] \tag{20c}$$

Acceleration of Wheel with Respect to Body

$$\ddot{z}_n = \ddot{r}_{nk} - \ddot{z}_o - \dot{\omega}_{oi}Y_n + \dot{\omega}_{oj}X_n \tag{16c}$$

Wheel Bounce

$$\ddot{r}_{nk} = \frac{1}{m_n}\left[G_{nk} - F_{nk} + m_n g\right] \tag{40c}$$

Suspension Force

$$F_{nk} = K_{ns}(z_n) + C_{ns}(\dot{z}_n)\phi_{ns}(z_n) \tag{60c}$$

Terrain-Elevation Function

$$r_{ngk} = f\left(t + \frac{Y_n}{V}\right) \tag{58c}$$

Tire Deflection

$$r_{nw} = r_{ngk} - r_{nk} \tag{59c}$$

Ground-Reaction Force

$$G_{nk} = K_{nw}(R_w + r_{nw}) + C_{nw}(\dot{r}_{nw})\phi_{nw}(R_w + r_{nw}) \tag{61c}$$

REFERENCES

1. I. J. Sattinger, E. B. Therkelsen, C. Garelis, and V. H. Geyer, Analysis of the Suspension System of the M47 Tank by Means of Simulation Techniques, Report Number 2023-2-T, Engineering Research Institute, The University of Michigan, Ann Arbor, Mich., June 1954 (UNCLASSIFIED).

2. E. M. Grabbe, S. Ramo, and E. E. Wooldridge, Handbook of Automation, Computation, and Control, Wiley, New York, N. Y., 1958, Vol. I, pp. 20-51.

3. J. L. Synge, B. A. Griffith, Principles of Mechanics, 2nd ed., McGraw-Hill, New York, N. Y., 1949.

4. H. Goldstein, Classical Mechanics, Addison-Wesley, Cambridge, Mass., 1950.

AD Div. 11/2

Willow Run Laboratories, U. of Michigan, Ann Arbor
COMPUTER SIMULATION OF VEHICLE MOTION IN THREE DIMENSIONS by I. J. Sattinger and D. F. Smith. May 60.
50 p. incl. illus., tables, 4 refs.
(Technical rept. no. 2901-10-T)
(Contracts DA-20-018-ORD-14658 and DA-20-018-ORD-19635)
Unclassified report

This report describes the results of a research program to develop techniques of simulating three-dimensional motion of a vehicle by means of electronic computers. In order to provide the basis for vehicle-motion simulation, a complete set of equations for a wheeled vehicle was developed, which permitted the analysis of motion in pitch, yaw, roll, bounce, surge, and sideslip. The derivation and summary of these equations is presented in this report. As a means of reducing the time and cost of computer solutions for certain restricted cases of vehicle motion, an investigation was made to determine to what extent simplifying assumptions could be made in these equations. A simplified set
(over)

UNCLASSIFIED

1. Vehicles — Motion
2. Mathematical computers — Applications
I. Sattinger, I. J. and Smith, D. F.
II. Ordnance Tank-Automotive Command
III. Contract DA-20-018-ORD-14658
IV. Contract DA-20-018-ORD-19635

Armed Services Technical Information Agency
UNCLASSIFIED

AD Div. 11/2

Willow Run Laboratories, U. of Michigan, Ann Arbor
COMPUTER SIMULATION OF VEHICLE MOTION IN THREE DIMENSIONS by I. J. Sattinger and D. F. Smith. May 60.
50 p. incl. illus., tables, 4 refs.
(Technical rept. no. 2901-10-T)
(Contracts DA-20-018-ORD-14658 and DA-20-018-ORD-19635)
Unclassified report

This report describes the results of a research program to develop techniques of simulating three-dimensional motion of a vehicle by means of electronic computers. In order to provide the basis for vehicle-motion simulation, a complete set of equations for a wheeled vehicle was developed, which permitted the analysis of motion in pitch, yaw, roll, bounce, surge, and sideslip. The derivation and summary of these equations is presented in this report. As a means of reducing the time and cost of computer solutions for certain restricted cases of vehicle motion, an investigation was made to determine to what extent simplifying assumptions could be made in these equations. A simplified set
(over)

UNCLASSIFIED

1. Vehicles — Motion
2. Mathematical computers — Applications
I. Sattinger, I. J. and Smith, D. F.
II. Ordnance Tank-Automotive Command
III. Contract DA-20-018-ORD-14658
IV. Contract DA-20-018-ORD-19635

Armed Services Technical Information Agency
UNCLASSIFIED

AD Div. 11/2

Willow Run Laboratories, U. of Michigan, Ann Arbor
COMPUTER SIMULATION OF VEHICLE MOTION IN THREE DIMENSIONS by I. J. Sattinger and D. F. Smith. May 60.
50 p. incl. illus., tables, 4 refs.
(Technical rept. no. 2901-10-T)
(Contracts DA-20-018-ORD-14658 and DA-20-018-ORD-19635)
Unclassified report

This report describes the results of a research program to develop techniques of simulating three-dimensional motion of a vehicle by means of electronic computers. In order to provide the basis for vehicle-motion simulation, a complete set of equations for a wheeled vehicle was developed, which permitted the analysis of motion in pitch, yaw, roll, bounce, surge, and sideslip. The derivation and summary of these equations is presented in this report. As a means of reducing the time and cost of computer solutions for certain restricted cases of vehicle motion, an investigation was made to determine to what extent simplifying assumptions could be made in these equations. A simplified set
(over)

UNCLASSIFIED

1. Vehicles — Motion
2. Mathematical computers — Applications
I. Sattinger, I. J. and Smith, D. F.
II. Ordnance Tank-Automotive Command
III. Contract DA-20-018-ORD-14658
IV. Contract DA-20-018-ORD-19635

Armed Services Technical Information Agency
UNCLASSIFIED

AD Div. 11/2

Willow Run Laboratories, U. of Michigan, Ann Arbor
COMPUTER SIMULATION OF VEHICLE MOTION IN THREE DIMENSIONS by I. J. Sattinger and D. F. Smith. May 60.
50 p. incl. illus., tables, 4 refs.
(Technical rept. no. 2901-10-T)
(Contracts DA-20-018-ORD-14658 and DA-20-018-ORD-19635)
Unclassified report

This report describes the results of a research program to develop techniques of simulating three-dimensional motion of a vehicle by means of electronic computers. In order to provide the basis for vehicle-motion simulation, a complete set of equations for a wheeled vehicle was developed, which permitted the analysis of motion in pitch, yaw, roll, bounce, surge, and sideslip. The derivation and summary of these equations is presented in this report. As a means of reducing the time and cost of computer solutions for certain restricted cases of vehicle motion, an investigation was made to determine to what extent simplifying assumptions could be made in these equations. A simplified set
(over)

UNCLASSIFIED

1. Vehicles — Motion
2. Mathematical computers — Applications
I. Sattinger, I. J. and Smith, D. F.
II. Ordnance Tank-Automotive Command
III. Contract DA-20-018-ORD-14658
IV. Contract DA-20-018-ORD-19635

Armed Services Technical Information Agency
UNCLASSIFIED

AD

of equations is contained in the report for cases in which surge can be neglected and angular motions in pitch and roll do not exceed 10°. A second simplified set of equations contains the further restriction that only pitch, bounce, and roll occur.

In order to establish justification for the simplified equations, an experimental program was carried out on an XM-151 military truck to determine its motion when traveling over certain road obstacles under specified conditions. The results were compared with those of corresponding runs in an analog-computer simulation. It was concluded that the simplified equations allowing only for pitch, bounce, and roll motion gave a satisfactory representation of the field-test data, but that improved correlation could be obtained by the simplified set of equations which accounted for lateral motion as well.

UNCLASSIFIED

UNITERMS

Vehicle
Motion
Analog computer
Simulation
Wheel
Pitch
Yaw
Bounce
Roll
Surge
Sideslip
Equation
Field test

UNCLASSIFIED

AD

of equations is contained in the report for cases in which surge can be neglected and angular motions in pitch and roll do not exceed 10°. A second simplified set of equations contains the further restriction that only pitch, bounce, and roll occur.

In order to establish justification for the simplified equations, an experimental program was carried out on an XM-151 military truck to determine its motion when traveling over certain road obstacles under specified conditions. The results were compared with those of corresponding runs in an analog-computer simulation. It was concluded that the simplified equations allowing only for pitch, bounce, and roll motion gave a satisfactory representation of the field-test data, but that improved correlation could be obtained by the simplified set of equations which accounted for lateral motion as well.

UNCLASSIFIED

UNITERMS

Vehicle
Motion
Analog computer
Simulation
Wheel
Pitch
Yaw
Bounce
Roll
Surge
Sideslip
Equation
Field test

UNCLASSIFIED